Global vegetation distribution driving factors in two Dynamic Global Vegetation Models of contrasting complexities

Li, Huan; Renssen, Hans; Roche, Didier M.

published in
Global and Planetary Change
2019

DOI (link to publisher)
10.1016/j.gloplacha.2019.05.009

document version
Publisher's PDF, also known as Version of record

Global and Planetary Change 180 (2019) 51–65

Contents lists available at ScienceDirect

Global and Planetary Change

journal homepage: www.elsevier.com/locate/gloplacha

Global vegetation distribution driving factors in two Dynamic Global Vegetation Models of contrasting complexities

Huan Li[a,*], Hans Renssen[a,b], Didier M. Roche[a,c]

[a] Department of Earth Sciences, VU University Amsterdam, De Boelelaan 1085, 1081 HV Amsterdam, The Netherlands
[b] Department of Natural Sciences and Environmental Health, University of South-Eastern Norway, 3800 Bø i Telemark, Norway
[c] Laboratoire des Sciences du Climat et de l'Environnement, IPSL, Laboratoire CEA-INSU-UVSQ-CNRS, Gif-sur-Yvette, France

ARTICLE INFO

Keywords:
Global vegetation responses
Mid-Holocene
CO_2 scenarios
DGVMs
Ecophysiological processes

ABSTRACT

This study compares the dynamic vegetation response in two Dynamic Global Vegetation Models (DGVMs) with contrasting processes complexity to changes in climate and atmospheric CO_2. We consider observed pre-industrial climates and four different simulated climate change states relative to preindustrial conditions: the mid-Holocene (6 ka), the pre-industrial state with halved CO_2 levels (140 ppm), doubled CO_2 (560 ppm), and quadrupled CO_2 (1120 ppm). The two DVGMs are LPJ-GUESS and VECODE. The input climate is derived from an earth system model of intermediate complexity (iLOVECLIM). We evaluate the sensitivities of these two DGVMs to changing climate and CO_2 levels and assess the impact of their respective complexity on these sensitivities. Our results show that both DGVMs yield results consistent with the broad features of pre-industrial vegetation dynamics and changes in vegetation from mid-Holocene to pre-industrial. They also agree with the patterns of vegetation responses to the more extreme varying CO_2 scenarios, yet with stronger magnitudes in LPJ-GUESS than in VECODE; in particular, large uncertainties are associated with the response of tropical vegetation to varying CO_2 levels. LPJ-GUESS simulates stronger positive responses of global net primary production (NPP) to elevated CO_2 levels than VECODE, particularly in tropical regions. The increase in global NPP differs by 8% between the two DGVMs under 2*CO_2 scenarios. Also, LPJ-GUESS simulates tropical vegetation sensitivities, defined here as the changes in tree-cover per degree of temperature anomaly, varying from 0.5 ($°C^{-1}$), 0.25 ($°C^{-1}$) to 0.15 ($°C^{-1}$) under ½*CO_2, 2*CO_2, and 4*CO_2 scenarios. In VECODE these values are around 0.05 ($°C^{-1}$) for all scenarios. The higher sensitivity of LPJ-GUESS to CO_2 concentration levels is likely related to the inclusion of more detailed ecophysiological processes. The two DGVMs' different complexity of eco-physiological processes also impacts on vegetation requirements for rainfall due to the physiological effects that more efficient water use of vegetation is facilitated under elevated atmospheric CO_2 concentration. The sensitivity of global Leaf Area Index (LAI) in the two DGVMs decreases with the increasing atmospheric CO_2 from pre-industrial level to 4*CO_2 scenario. The uncertainties of vegetation simulations are mainly contributed by the tropical vegetation response to climate and CO_2 concentration due to the inclusion of ecosystem processes in both DGVMs and the scheme of vegetation classification. Based on our results, we recommend to use a standard set of vegetation types and to set up systematic simulations detecting the range of vegetation sensitivity to varying CO_2 and climate forcing when inter-comparing different DGVMs.

1. Introduction

Vegetation is one of the important components of the climate system, whose distribution is broadly correlated with other components in the climate system. For instance, as temperature rises, the amounts of snow and ice reduce in the taiga and tundra transition regions. Taiga would then progressively replace tundra towards higher latitudes. Similarly, the moisture-limited transitions between forest, savanna and desert (Mayle et al., 2007) are sensitive to seasonal and annual precipitation (Furley et al., 1992). Vegetation also affects the regional climate and the Earth's carbon cycle (Bonan, 2008) in many ways through interactions with the atmosphere, e.g., through the modifications of land albedo, evapotranspiration, photosynthesis, productivity, competition, and disturbances (Denman et al., 2007). Using the same taiga regions' evolution as an example, a warmer climate would be reinforced following a transition from tundra to taiga since the albedo

* Corresponding author.
E-mail address: h.li@vu.nl (H. Li).

https://doi.org/10.1016/j.gloplacha.2019.05.009
Received 10 August 2018; Received in revised form 17 May 2019; Accepted 22 May 2019
Available online 25 May 2019
0921-8181/

of the latter (about 0.2) is lower (Harding and Pomeroy, 1996; Pomeroy and Dion, 1996; Hedstrom and Pomeroy, 1998), allowing the taiga-covered land surface to absorb more solar radiation. Additionally, CO_2 concentration also interacts with climate and vegetation (Ciais et al., 1997). For instance, Zhu et al. (2016) found that CO_2 fertilization effects explain 70% of the observed greening trend during 1982–2009, especially in tropical regions. On the other hand, climate feeds back on CO_2 concentration through the release/uptake of CO_2 from land/ocean (Friedlingstein and Prentice, 2010; Liu et al., 2014; Wenzel et al., 2014). Overall, climate affects vegetation through plant-level processes (Badeck et al., 2004). In turn, vegetation feedbacks to climate through both plant-level and ecosystem-level processes (Friedlingstein et al., 2014). However, the interactions among vegetation, climate and CO_2 concentrations are rather complex due to several processes related to the exchange of turbulent fluxes of energy, water, momentum, and trace gases (Arora, 2002; Pitman, 2003).

Dynamic global vegetation models (DGVMs) have become fundamental tools to analyze these complex vegetation dynamics and interactions with climate and CO_2, being not only able to account for the interaction of biophysical, biochemical and eco-physiological processes, but also allowing to vary and analyze the effect of any one impact factor at a time. A number of DGVMs have been developed, e.g., CARAIB (Warnant et al., 1994), VECODE (Brovkin et al., 1997), LPJ-GUESS (Smith et al., 2001), LPJ-DGVMs (Sitch et al., 2003), TRIFFID (Cox, 2001; Hughes et al., 2006), Hyland (Levy et al., 2004), ORCHIDEE (Krinner et al., 2005), aDGVM (Scheiter and Higgins, 2009), JSBACH (Raddatz et al., 2007; Brovkin et al., 2009; Reick et al., 2013), LPX-DGVM (Prentice et al., 2011), etc. They have been widely used to investigate past and future vegetation dynamics, and to estimate their interactions with climate and CO_2 concentrations. For instance, Brovkin et al. (2002) simulated the global carbon cycle, vegetation and climate dynamics during the Holocene within a climate system model (CLIMBER-2), in which the vegetation and carbon cycle are simulated in VECODE. Roche et al. (2007) simulated the distribution of potential natural vegetation (PNV) during the last glacial maximum (LGM) using VECODE to analyze the vegetation responses to cold climate and low CO_2 levels conditions. In addition, the contributions of low CO_2 concentration and climate to this LGM vegetation were studied using both ORCHIDEE (Woillez et al., 2011) and JSBACH (Claussen et al., 2013). An example of a study of warm climate conditions is provided by Woodward and Lomas (2004), who used the Sheffield DGVM (SDGVM) to show that a general decline in the terrestrial carbon sink can happen under global warming scenarios. Moreover, Kleinen et al. (2016) modelled interglacial carbon cycle dynamics in CLIMBER-2 (Petoukhov et al., 2000; Ganopolski et al., 2001) coupled to the LPJ-DGVM to detect the impacts of slow carbon processes (peat accumulations and $CaCO_3$ accumulations in shallow water) on CO_2 concentration during three interglacials. Also, Higgins and Scheiter (2012) pointed out that increasing atmospheric CO_2 concentration will force transitions to vegetation states characterized by higher biomass and/or woody plant dominance based on simulations in aDGVM.

DGVMs have different sensitivities to climate and CO_2 levels, which in turn is related to the dissimilar complexities, associated with alternative parameterizations and diverse inclusions of processes (Prentice et al., 2007). These differences bring uncertainties during simulations, which might have strong impacts on the simulated vegetation responses to climate change (Friedlingstein et al., 2006; Sitch et al., 2008). To evaluate the model-related uncertainties, several studies started to use multiple DGVMs simulating vegetation dynamics and feedbacks. Cramer et al. (2001) first studied the global responses of terrestrial ecosystem structure and function to CO_2 and climate change using six DGVMs. In this study, the mean result of the six DGVMs shows a fair agreement with observed pre-industrial vegetation as measured by Kappa statistics and it is then used to analyze global vegetation responses and feedbacks. Moreover, Friedlingstein et al. (2006) studied the coupling between climate change and carbon cycle using eleven coupled climate-carbon cycle models. They found large inter-model differences of both land and ocean carbon cycle sensitivity to future climates among the eleven models and supported the view that analyses with an ensemble of independent models are preferable to assess the uncertainties related to model structure and parameter choices. Likewise, Sitch et al. (2008) modelled the contemporary and future global carbon cycle using five DGVMs and evaluated them by comparing the simulation results. Their study indicates that major DGVM uncertainties are related to NPP responses to tropical climates and soil respiration responses to extra-tropical climates. Similarly, Galbraith et al. (2010) looked at the mechanism of biomass loss in the Amazon using three DGVMs (LPJ (Smith et al., 2001; Sitch et al., 2003), Hyland (Levy et al., 2004) and TRIFFID (Cox, 2001)) and concluded that these three DGVMs simulated reductions in biomass through different mechanisms. Furthermore, Friend et al. (2014) analyzed possible vegetation responses to future climate using seven DGVMs and highlighted the importance of uncertainties in projected changes in carbon residence time due to the different formulations in DGVMs.

Although these multiple-DGVM studies have revealed many important differences between the vegetation simulations, these differences have not been systematically evaluated yet. Such a systematic evaluation would require experiments with various DGVMs, forced by different identical climatic conditions and CO_2 concentrations, which could reveal differences in sensitivity to these conditions in various models due to their varying importance and parameterizations of fundamental physiological processes (Quillet et al., 2010). However, setting up a full-scale model-intercomparison project would take a considerable effort, as it requires involvement of many modelling groups and allocation of substantial computer resources. Thus, a first step is to perform such an evaluation with two models at extreme ends of the complexity range, i.e., a reduced form and complex DGVM, so that we could have a basic understanding of how much the DGVMs' complexity impacts on their sensitivity to climates and CO_2 concentrations.

Therefore, we here make controlled comparisons between the responses of two DGVMs that are positioned at opposite sides of the complexity range: VECODE (Brovkin et al., 1997), a relatively simple model, and LPJ-GUESS (Smith et al., 2001; Sitch et al., 2003), a comprehensive DGVM. We expose them to identical sets of climate change scenarios. Initially, the two DGVMs are both run with observed pre-industrial climatology and atmospheric CO_2 concentration. They are then run under four climate change states as test beds. These climate states are derived from simulations performed with the iLOVECLIM climate model (Goosse et al., 2010; Roche et al., 2014), including one simulation with realistic forcing from the mid-Holocene (6 ka) and three idealized simulations with half, twofold and fourfold the pre-industrial CO_2 concentration (i.e., $½*CO_2$, $2*CO_2$, $4*CO_2$). In the following, we address three main questions: 1) are the two DGVMs able to simulate pre-industrial vegetation dynamics; 2) how sensitive are the vegetation dynamics to climate and atmospheric CO_2 changes in the two DGVMs; and 3) what are the relative uncertainties in simulating vegetation dynamics and functions associated with different choices of DGVMs?

2. Methods: model description and experimental design

2.1. Dynamic global vegetation models (DGVMs)

We apply two DGVMs in this study: the Vegetation Continuous Description Model (VECODE, Brovkin et al., 1997) and the Lund-Potsdam-Jena General Ecosystem Simulator (LPJ-GUESS, Smith et al., 2001; Sitch et al., 2003). Since these models have been extensively described elsewhere (Brovkin et al., 1997; Smith et al., 2001; Sitch et al., 2003), we only summarize the essential model characteristics in the following.

LPJ-GUESS is designed primarily as a dynamical vegetation model with explicit scaling of individual-level processes among several

patches (15 patches in this study) in each grid cell, employing biophysical and physiological process parameterizations identical to the equilibrium model BIOME3 (Haxeltine and Prentice, 1996). The patches are corresponding to the maximum influencing area of one large full-grown individual (trees in most cases) on its neighbors. LPJ-GUESS adds dynamic representations of establishment, mortality, growth, carbon allocation, plant allometry and dynamic competition among 11 plant functional types (PFTs), and simulates photosynthesis, plant distribution and competition among them. Those physiological processes are simulated on a daily time step. The net primary production (NPP) is allocated to the leaves, sapwood and roots for each PFT in each cohort at the end of simulation year (Smith et al., 2001). LPJ-GUESS requires climatic inputs (including monthly temperature, precipitation and cloud cover) and CO_2 forcing. The diffusion of CO_2 into the leaf varies with atmospheric CO_2, resulting in changing plant photosynthesis and stomatal regulation through biochemical and hydrological mechanisms (Hickler et al., 2008). PFT-specific parameters govern competition for light and water among PFTs. Soil hydrology influencing both plant and soil behaviors depends on the prescribed soil texture and vegetation biophysical processes.

In contrast, VECODE is a reduced-form DGVM, designed directly for inclusion in earth system models (Brovkin et al., 1997), including simple (implicit) eco-physiological processes among 2 plant functional types (PFTs). VECODE also uses physiological formulations simulating the vegetation dynamical competitions, mortality and C allocation but in an implicit way, i.e., these only depend on bioclimatic constraints. Vegetation dynamics in VECODE are described using 2 PFTs (tree, grass, and a dummy PFT: bare ground) in annual time step, and these 2 PFT fractions with bare soil amount to 1.0 in each grid cell. It requires climatic inputs including annual temperature, precipitation and gdd0 (growing day degrees above 0 °C), and CO_2 forcing which is a biotic growth factor in a logarithmic form (den Elzen et al., 1995) related to the NPP calculation among PFTs. Similar to LPJ-GUESS, soil hydrology in VECODE also depends on the prescribed soil texture and vegetation biophysical processes, influencing both plant and soil behaviors, but it is kept constant during offline simulations.

Vegetation dynamics in these two DGVMs are based on annual net primary production (ANPP) and biomass growth. Both of them include competition and probabilities of natural disturbances among PFTs which are assigned different parameterizations with respect to eco-physiological processes and are used to define the structural characteristics of vegetation (Woodward and Cramer, 1996; Cramer, 1997). They simulate the process-based terrestrial vegetation dynamics via physiological, biogeophysical and biogeochemical processes, but the degree of complexity in mechanistic representation of these processes is different. Hereafter, we focus on two aspects of their differences regarding vegetation dynamics: the breakdown between PFTs and the ecophysiological processes.

2.2. Vegetation classification scheme for PFTs

In order to compare modelled vegetation dynamics among PFTs by the two DGVMs and independent gridded global potential natural vegetation (PNV) based on BIOME 6000 dataset (Levavasseur et al., 2012), we convert them to very broadly defined vegetation types (Table 2) from their different PFTs using a classification scheme.

Several classification schemes have been applied in previous studies, based on different attributes of defined vegetation types (Cramer et al., 2001; Joos et al., 2004; Hickler et al., 2006; Schurgers et al., 2006; Prentice et al., 2011; Smith et al., 2014; Dallmeyer et al., 2019). For instance, Cramer et al. (2001) applied a classification scheme based on biomass and leaf area index (LAI) values. Likewise, Hickler et al. (2006) and Smith et al. (2014) transferred distributions among 11 PFTs to 18 vegetation types based on LAI classification rules to compare with their reference PNV distributions (Haxeltine and Prentice, 1996). Moreover, classification schemes using the foliage projective cover (FPC) of PFTs (Schurgers et al., 2006) or the combination of FPC and stand height (Joos et al., 2004; Prentice et al., 2011; Calvo and Prentice, 2015; Kageyama et al., 2013) are also widely used to produce PNV or dominant vegetation types. In previous studies, the number of determined vegetation types in PNV is always decided by their referred PNV dataset for pre-industrial vegetation comparisons, including downscaling from 9 PFTs to 12 biomes in LPX (Prentice et al., 2011; Calvo and Prentice, 2015), from 10 PFTs to 12 biomes in ORCHIDEE (Kageyama et al., 2013) and upscaling from 10 PFTs to 6 biomes in ORCHIDEE (Woillez et al., 2011) and from 11 PFTs to 7 biomes in LPJ-DGVM (Schurgers et al., 2006). However, these classification schemes are related to comparisons between two objects, i.e., one modelled PNV (whether PNV simulated by one model or PNV summarized from multiple models simulations) and one referred PNV, therefore not ideal for our study involving comparisons among three datasets, i.e. two modelled PNV distributions and one reference PNV dataset. Most recently, Dallmeyer et al. (2019) suggested a classification scheme to harmonize simulated PFT distributions to nine mega-PFTs using the minimum PFT fractions and a few bioclimatic factors. Their scheme is a simple but powerful method for biomisation for PFTs distributions, but we here mainly focus on tree and grass in relation to different climate conditions.

Because of the unsuitability of these schemes, we thus defined a new classification scheme based on FPC suitable for the two models and the reference PNV dataset for comparison purposes between them. We assign our simulated PFTs abundances and that in reference PNV dataset to the two dominant PFTs groups based on FPC keeping in line with VECODE. The modelled FPC among PFTs is used during this conversion since they can be derived directly from both LPJ-GUESS and VECODE output, without introducing much additional uncertainty. We upscaled the 11 PFTs in LPJ-GUESS and 8 biomes in Levavasseur et al. (2012) to 2 PFTs, avoiding the large uncertainties incurred by downscaling the smaller number of PFTs in VECODE to a higher number. During this process, we first convert modelled vegetation dynamics in LPJ-GUESS to PNV based on the scheme presented by Schurgers et al. (2006), after which we combined them to defined vegetation types (Table 2). Then, we produce the vegetation distributions using dominant vegetation types (here 2 PFTs and desert) which are calculated based on the fractions of vegetation types in each grid cell. The impacts of using this classification scheme are discussed further in Section 4.1.

2.3. The earth system model (iLOVECLIM) and climatic forcing

We use the atmosphere-sea ice-ocean-vegetation (ECBilt-CLIO-VECODE) components of iLOVECLIM (i.e. an updated version of LOVECLIM 1.2, Goosse et al., 2010, Roche et al., 2014) to simulate climates involving dynamical vegetation feedbacks, and we use only the atmosphere-sea ice-ocean (ECBilt-CLIO) components with prescribed vegetation to simulate climates excluding impacts of dynamical vegetation. ECBilt is the atmospheric component, consisting of a three-level, quasi-geostrophic model at T21 resolution (Opsteegh et al., 1998). In ECBilt, cloudiness is prescribed according to present-day climatology (Rossow et al., 1996). The surface albedo is a function of the fraction of the grid box covered by ocean, sea ice, trees, desert and grass (Goosse et al., 2010). The surface temperature and the development of snow cover are computed by performing the heat budget calculation over a single soil layer. Soil moisture is computed in a simple bucket model, in which the maximum water volume of the bucket is a function of the vegetation cover, i.e. it depends on the combination of three PFTs' cover. The sea ice-ocean part (CLIO) consists of a three dimensional, free surface ocean general circulation model coupled to a dynamic-thermodynamic sea-ice model (Goosse et al., 2010). The horizontal resolution of CLIO is 3° latitude by 3° longitude, and there are 20 unevenly spaced vertical layers in the ocean. CLIO provides ECBilt with the sea surface and sea-ice temperature, the fraction of sea ice in each ocean grid cell as well as the sea-ice and snow thickness. ECBilt gives CLIO the wind stresses, the

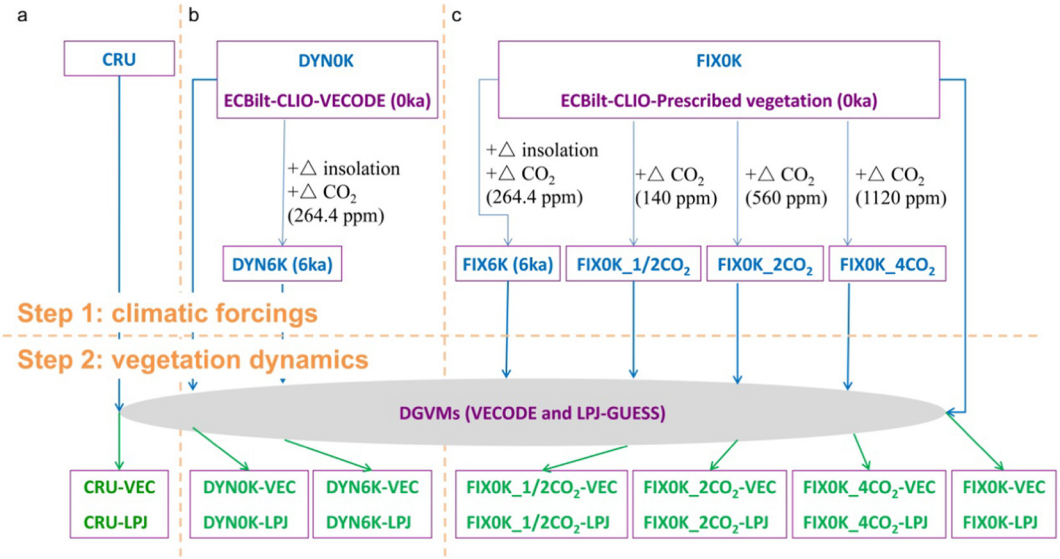

Fig. 1. Experimental set-up for the offline pre-industrial, the past climate change, and the CO_2 scenarios simulations. a, The control pre-industrial experiments: the two DGVMs are forced with observed pre-industrial climates (CRU dataset, 1901–1930) and annual global atmospheric CO_2 (280 ppm), at iLOVECLIMT21 resolution. b, The mid-Holocene experiments: the two DGVMs are driven by simulated mid-Holocene (DYN6K) and pre-industrial (DYN0K) climatologies respectively. c, the CO_2 scenarios experiments: the two DGVMs are run under simulated pre-industrial climates with pre-industrial CO_2 concentration (280 ppm) and three different settings of CO_2 levels (i.e. ½*CO_2: 140 ppm, 2*CO_2: 560 ppm, and 4*CO_2: 1120 ppm).

shortwave and net heat flux over the ocean and sea-ice over as well as the precipitation. Within iLOVECLIM, the vegetation dynamics in response to climate is simulated by VECODE (Brovkin et al., 1997). In turn, the surface albedo related to vegetation cover calculated by VECODE is passed to ECBilt. In some of our simulations VECODE was deactivated the vegetation characteristics being then were prescribed.

2.4. Experimental designs and data processes

We grouped all simulations in three classes: the control pre-industrial simulations, the mid-Holocene simulations, and the CO_2 scenario simulations (Fig. 1). Simulations in each class include two steps: 1) preparation of the climatic forcing, 2) simulation of vegetation in both DGVMs.

2.4.1. Control pre-industrial experiments (Fig. 1a)

In the first set of experiments, both DGVMs are run under observedpre-industrial climates and annual global atmospheric CO_2 (280 ppm), at iLOVECLIM T21 resolution. Observed climatologies are monthly means for the period 1901–1930 from the University of East Anglia Climate Research Unit (CRU) gridded dataset (New et al., 2000). These climatologies are represent active of the pre-industrial climates since the temperature in the early 20th century had not risen so much yet and it was close to the pre-industrial state (IPCC, 2014). For LPJ-GUESS, we keep N deposition (1 kgN/ha/year) constant. These control runs are named CRU-VEC and CRU-LPJ. Agreement between these simulated vegetation and independent global pre-industrial natural vegetation distributions (Levavasseur et al., 2012) are quantified using the kappa statistic (Monserud and Leemans, 1992) and matching ratios. The kappa statistic is derived by subtracting the overall proportion of agreement between two maps and normalizing the result normalized by the maximum possible different value (Prentice et al., 1992). The statistic is close to zero when agreement is no better than random and it reaches unity when agreement is perfect. It has been used as an objective tool for comparing global vegetation maps in several previous studies (Monserud and Leemans, 1992; Haxeltine and Prentice, 1996; Cramer et al., 2001; Hickler et al., 2006). The matching ratio is defined as the percentage of gridcells that simulated dominant PFTs (grass, trees or desert) matching Levavasseur's PNV distribution, it is an indicator of the agreement of individual vegetation types between our two simulated vegetation and reference PNV dataset.

2.4.2. Mid-Holocene experiments (Fig. 1b)

The two DGVMs are driven by simulated mid-Holocene (DYN6K) and pre-industrial (DYN0K) climatologies (the last 30-year mean climates) derived from iLOVECLIM, using the forcing shown in Table 1. These climatologies were obtained with an iLOVECLIM-version that included a dynamically ('DYN') coupled VECODE, thus comprising vegetation-climate feedbacks. The spin-up process of these climate simulations was taken to be 1000 years. The four runs are named DYN0K-VEC, DYN0K-LPJ, DYN6K-VEC, and DYN6K-LPJ. Comparisons between these runs allow assessing impacts of the two models' complexity on the vegetation dynamics between 6 ka and 0 ka.We designed additional experiments to simulate climates with fixed, prescribed vegetation under pre-industrial conditions, of which the climatic results are named FIX0K, to analyze the impacts of dynamical vegetation feedbacks during comparisons between the two DGVMs. This fixed vegetation (i.e., ECBilt-CLIO with VECODE deactivated) is derived from the CMIP LUH2 dataset (http://luh.umd.edu/data.shtml), at 850 CE. The comparison between FIX0K and DYN0K allows assessing the role of dynamical vegetation in iLOVECLIM. Afterwards, two additional experiments (FIX0K_VEC and FIX0K_LPJ), i.e., simulations in both DGVMs driven by climates in FIX0K, are run to prepare the baselines of vegetation dynamics for the CO_2 scenarios experiments.

2.4.3. CO_2 scenarios experiments (Fig. 1c)

The two DGVMs are driven by simulated climates (the last 30-year-

Table 1
Earth's orbital parameters and trace gases from PMIP4.

Period	Orbital forcing	Greenhouse Gas
Pre-industrial (0 ka)	Eccentricity: 0.0167724; Obliquity: 23.446; Angular precession: 102.04	CO_2 = 280.0 ppm; CH_4 = 760.0 pbm; N_2O = 270.0 pbm
Mid-Holocene (6 ka)	Eccentricity: 0.018682; Obliquity: 24.105; Angular precession: 0.87	CO_2 = 264.4 ppm; CH_4 = 579.0 pbm; N_2O = 262.0 pbm

mean climatologies) in iLOVECLIM under pre-industrial forcing with three different settings of CO_2 levels (i.e. ½*CO_2: 140 ppm, 2*CO_2: 560 ppm, and 4*CO_2: 1120 ppm).The three climate simulations (FIX0K_½CO_2, FIX0K_2CO_2, and FIX0K_4CO_2) are continuations of FIX0K, and include fixed, prescribed 0 ka vegetation. The spin up process of FIX0K_½CO_2 and FIX0K_2CO_2 took 1000 years and that of FIX0K_4CO_2 2000 years. These six experiments, comprising all combinations of the three climate states with the two DGVMs, are named FIX0K_½CO_2-VEC, FIX0K_½CO_2-LPJ, FIX0K_2CO_2-VEC, FIX0K_2CO_2-LPJ, FIX0K_4CO_2-VEC, and FIX0K_4CO_2-LPJ. For each DGVM, all vegetation simulations under CO_2 scenarios are compared with its baseline (either FIX0K_VEC or FIX0K_LPJ), determining their responses to different levels of climate and CO_2changes. Analyses are based on 30-year averages that are derived from the last 30 years of each simulation. The reasons for their differences in vegetation dynamics are complex, we here focus on their sensitivity to temperature, precipitation and CO_2-levels. The sensitivity to temperature is defined as changes in tree-cover per degree of temperature anomaly between CO_2 scenarios and FIX0K.

3. Results and discussion

We focus on simulated vegetation under different climate conditions in the two DGVMs in this section. The simulated climate conditions are presented in supplementary information.

3.1. Pre-industrial vegetation

The two DGVMs capture the major features of the modern PNV distribution (Levavasseur et al., 2012) when forced with observed climatology (Fig. 2a, b, c) in experiments CRU-VEC and CRU-LPJ. They produce a forest belt in mid-to-high latitudes (Siberia, Europe, and eastern North America); subtropical deserts in Africa and Eurasia; subtropical grassland and tropical forest in southeastern Asia, central Africa as well as South America. The DGVMs also capture the northern tree line correctly, with the exception of eastern Siberia, where a more southerly transition zone to Arctic tundra is predicted. However, they both simulate more vegetation in the Middle East but less in western Greenland and southwestern North America. They agree less in desert distribution simulations (difference up to 20%). This mismatch is related to a larger extension of mid-latitude grass in VECODE than in reference dataset and an underestimation of desert in LPJ-GUESS.

For each DGVM, the matching ratio (Fig. 2d, e) is consistent with their dominant PFT distributions, slightly higher in VECODE (67%) than in LPJ-GUESS (61%). The overall value of the kappa statistic was 0.47 in VECODE, which indicates a fair agreement (Monserud and Leemans, 1992) with the reference PNV dataset, while it is a bit lower at 0.37 in LPJ-GUESS, indicating a lower level of agreement. The two models perform similarly in Eurasia (matching ratio of about 70%) and South America (about 75%). In Australia, an underestimation in desert cover contributes to the lowest matching ratio (50%) of all continents in both models. VECODE has higher matching ratios in North America (65%) and Africa (55%) by about 10% than LPJ-GUESS due to its more accurate desert distribution (60% matched) compared with 40% in LPJ-GUESS (Fig. 2e). However, it should be noted that the grass-desert transitions, in particular in tropical regions, are not well represented in our classification scheme. An arbitrary aggregation from 11 PFTs to 2 PFTs in LPJ-GUESS involves underestimations in desert distribution which is related to the low threshold of 0.2 for the combined FPC of grass and desert (Schurgers et al., 2006). In addition, the PNV (Levavasseur et al., 2012) involves uncertainties especially in transition zones during classification and upscaling processes.

3.2. Vegetation from mid-Holocene to pre-industrial

Compared with the simulated pre-industrial vegetation (DYN0K-LPJ and DYN0K-VEC) in both DGVMs, vegetation covers, LAI and NPP increase (Fig. 3) at 6 ka (DYN6K-LPJ and DYN6K-VEC) in Northern Africa, the Middle East, and northern high latitudes, with stronger vegetation responses in LPJ-GUESS in mid-latitudes. The significant rise in

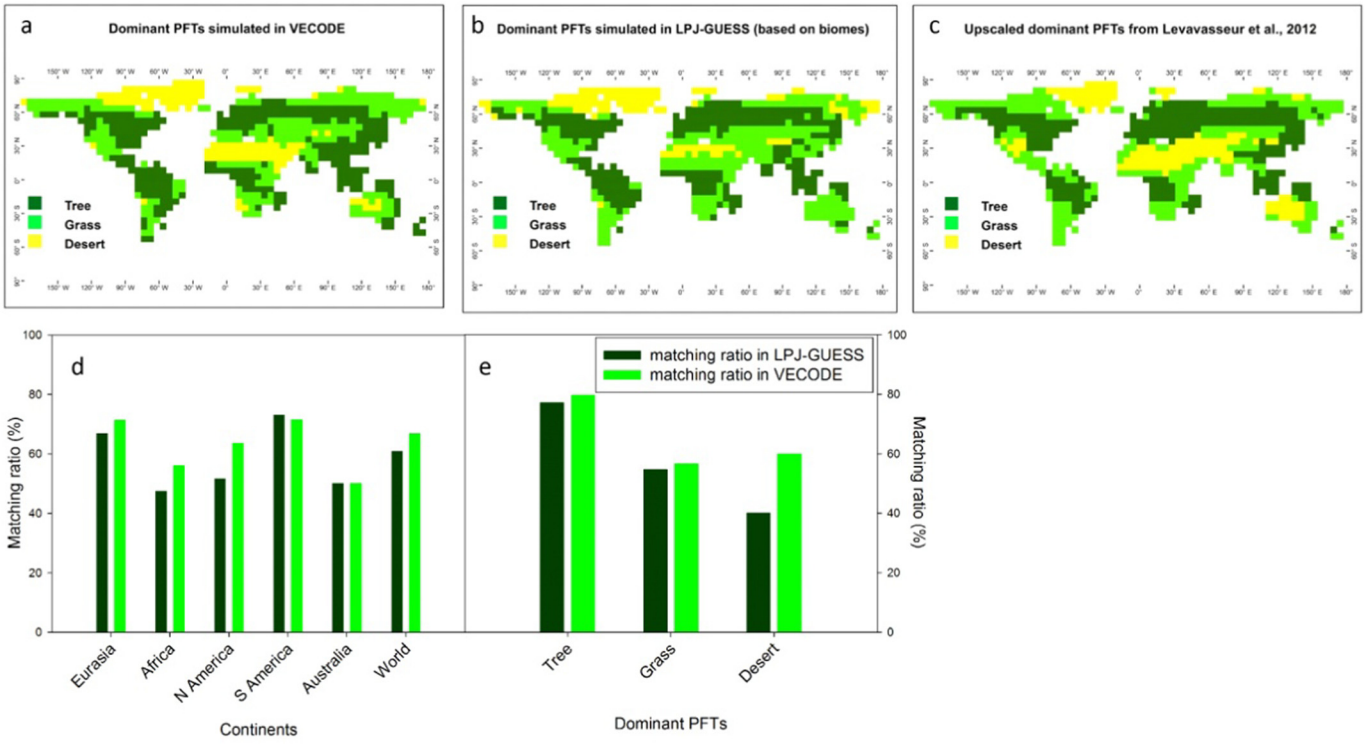

Fig. 2. Simulated pre-industrial potential natural vegetation distributions for two aggregated PFTs (tree and grass) in VECODE (a, CRU-VEC) and in LPJ-GUESS (b, CRU-LPJ), and upscaled reference PNV distribution (c). Matching ratios of the two models in continents (d) and aggregated PFTs (e).

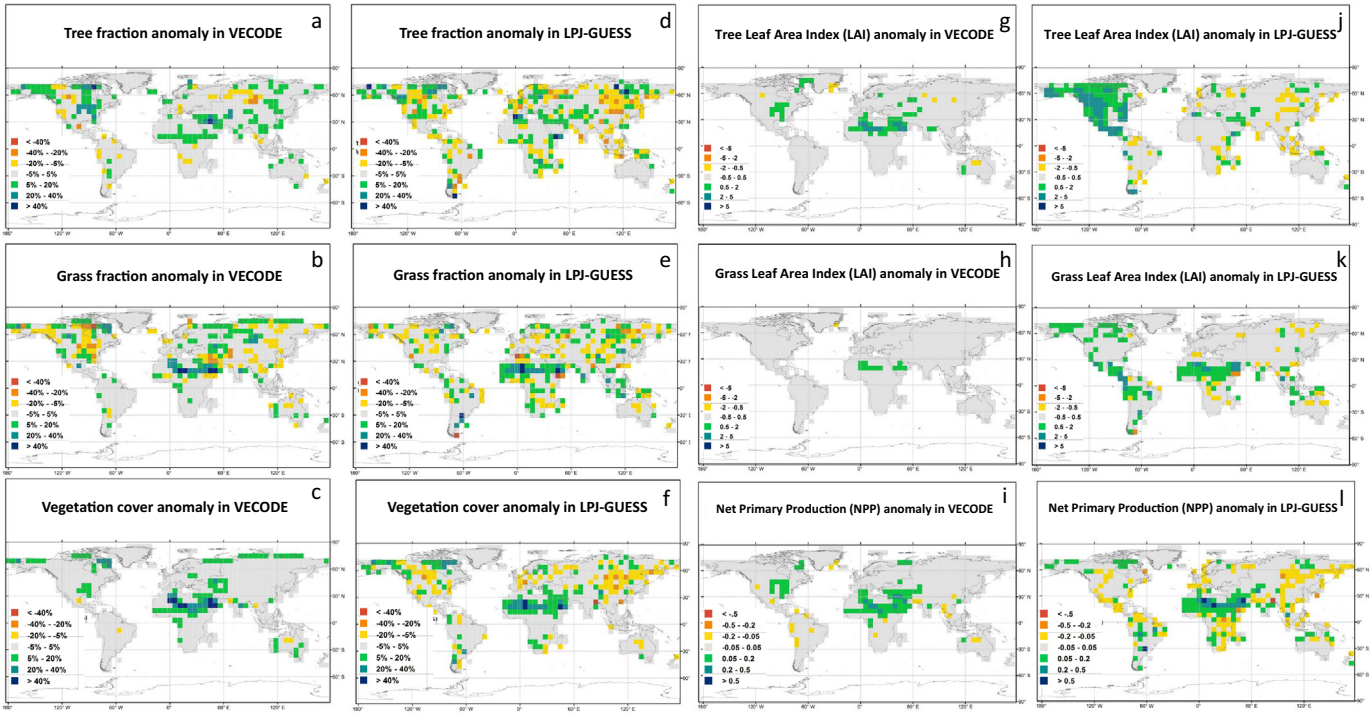

Fig. 3. Changes in vegetation coverage (%) and LAI (m^2/m^2) for aggregated PFTs, total vegetation cover and NPP ($kgC/yr/m^2$) between mid-Holocene (6 ka, DYN6K) and pre-industrial (0 ka, DYN0K) in VECODE (DYN6K-VEC and DYN0K-VEC) and LPJ-GUESS (DYN6K-LPJ and DYN0K-LPJ).

vegetation-cover (5% in LPJ-GUESS and 7% in VECODE, Fig. 3c, f) in Northern Africa contributed by the higher grass-cover is associated with more intensive precipitation (> 100%) induced by strengthened African summer monsoon in the mid-Holocene. Likewise, higher vegetation-cover in the Middle East is primarily a consequence of more (about 140% compared to pre-industrial condition) precipitation due to stronger Indian summer monsoon induced by higher summer insolation. In contrast, the approximate 3% increases in poleward of 60 N tree-cover (Fig. 3a, d) reflect the expansion of boreal forest into the area previously covered by tundra, especially in Eastern Siberia, northwestern and northeastern North America, relating to a more active growing season due to the enhanced summer warmth (see appendix) in the mid-Holocene. The LAI (Fig. 3g, h, j, and k) and NPP (Fig. 3i, l) are consistent with vegetation cover anomalies (Fig. 3a–f) between 6 ka and 0 ka. These simulated vegetation changes between 6 ka and 0 ka are consistent with many previous results, including the increase of vegetation cover in North Africa and the Middle East (Claussen and Gayler, 1997; Prentice et al., 2000; Renssen et al., 2006; Dallmeyer et al., 2010; Goosse et al., 2010), and also the expansion of northern tree cover (Crucifix et al., 2002; Brovkin et al., 2002; Gallimore et al., 2005). In addition, a discrepancy of western North African vegetation cover in the mid-Holocene between our simulation (DYN6K-VEC) and Renssen et al. (2006) suggests impacts of different climate model versions on the vegetation simulations. In our version, the coupling between VECODE and ECBilt is updated through both surface albedo and soil hydrology (Goosse et al., 2010) rather than only the surface albedo as in Renssen et al. (2006). This more complete coupling resulted in different distribution of precipitation in Northern Africa, leading to more greening in eastern part (Goosse et al., 2010).

VECODE simulates a slight change in mid-latitude vegetation cover due to the increase in grass-cover often at the expense of tree cover, whereas LPJ-GUESS simulates about 5% decreased mid-latitude vegetation cover, mainly due to decreased tree-cover (5%–20%) in northwestern China and decreased grass-cover (also about 5%–20%) in southern Europe & central North America. The declined tree-cover in northwestern China is attributed to the −10% to −30% decreases in precipitation, showing that LPJ-GUESS is sensitive to precipitation in particular in water-limited regions, consistently with Galbraith et al. (2010).

3.3. Vegetation under different CO_2 level scenarios

As expected, the colder and drier climate of FIX0K_½CO_2 generates decreases in global tree cover (Fig. 4a, d) and increases in grass cover (Fig. 4b, e) in both DGVMs, in particular in the tropics. However, LPJ-GUESS simulates clearly stronger vegetation responses (Fig. 4) than VECODE. It simulates a marked reduction (by about 20%) in global tree-cover, with replacement by grass in tropics and reductions in boreal regions, leading to a 15% decrease in global vegetation cover. In contrast, VECODE simulates only about 3% decrease in global vegetation cover, due to less (about 8%) northern high latitude trees and slightly higher (about 2%) tree cover at mid-latitudes (Central North America, Western Europe, Central Asia and Eastern China). The changes in LAI and NPP are consistent with vegetation cover, with more significant increase in tropical grass LAI and NPP in LPJ-GUESS than VECODE. Compared with pre-industrial condition, LPJ-GUESS simulates much less reduction (11%) in global NPP under ½*CO_2 scenario than during LGM as modelled by LPX (28%, Prentice et al., 2011) the 31% declines in VECODE is of the same order as LPX. Moreover, LPJ-GUESS sees a stronger decrease (85%) in tropical tree LAI than in Amazon tree-LAI (about 29% to 44%) simulated by ORCHIDEE for the LGM climate (Woillez et al., 2011). As a result, the less reduced global NPP in LPJ-GUESS is due to the 22% increases in tropical NPP, which is attributed to the marked extension of tropical grass (Fig. 4e, k, l) due to its stronger competitiveness under halved CO_2 concentration, but this is hardly captured by VECODE with its small CO_2 dependence. However, the ½*CO_2 scenario is warmer and has lower CO_2 level than the LGM conditions, which weakens the competition of C3 plants (Cowling and Sykes, 1999; Cowling et al., 2001; Bond et al., 2003; Cowling and Shin, 2006), leading to this stronger reduction in tropical trees than seen in LGM studies (e.g., Woillez et al., 2011).

In contrast, compared to the baseline (FIX0K), the two DGVMs

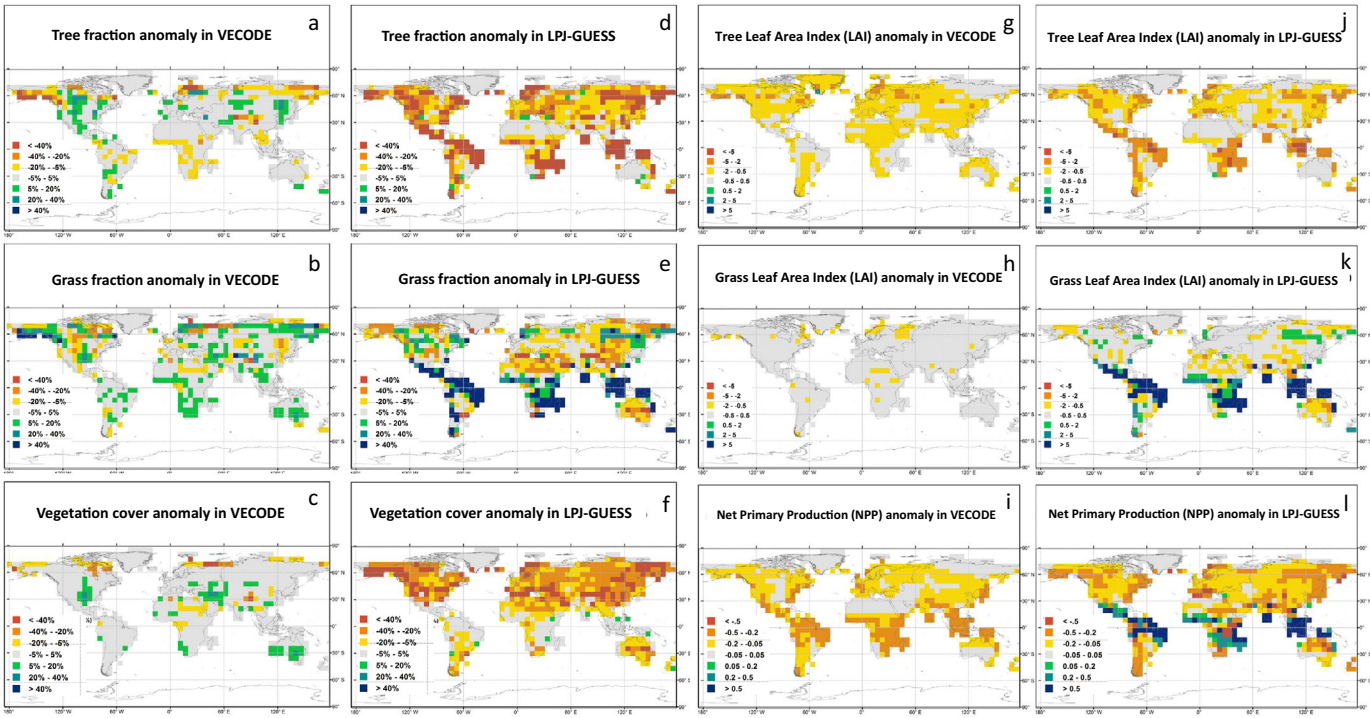

Fig. 4. Changes in vegetation coverage (%) and LAI (m^2/m^2) for aggregated PFTs, total vegetation cover and NPP (kgC/yr/m^2) under climate change (FIX0K_½CO_2 - FIX0K) in VECODE (FIX0K_½CO_2-VEC and FIX0K-VEC) and LPJ-GUESS (FIX0K_½CO_2-LPJ and FIX0K-LPJ).

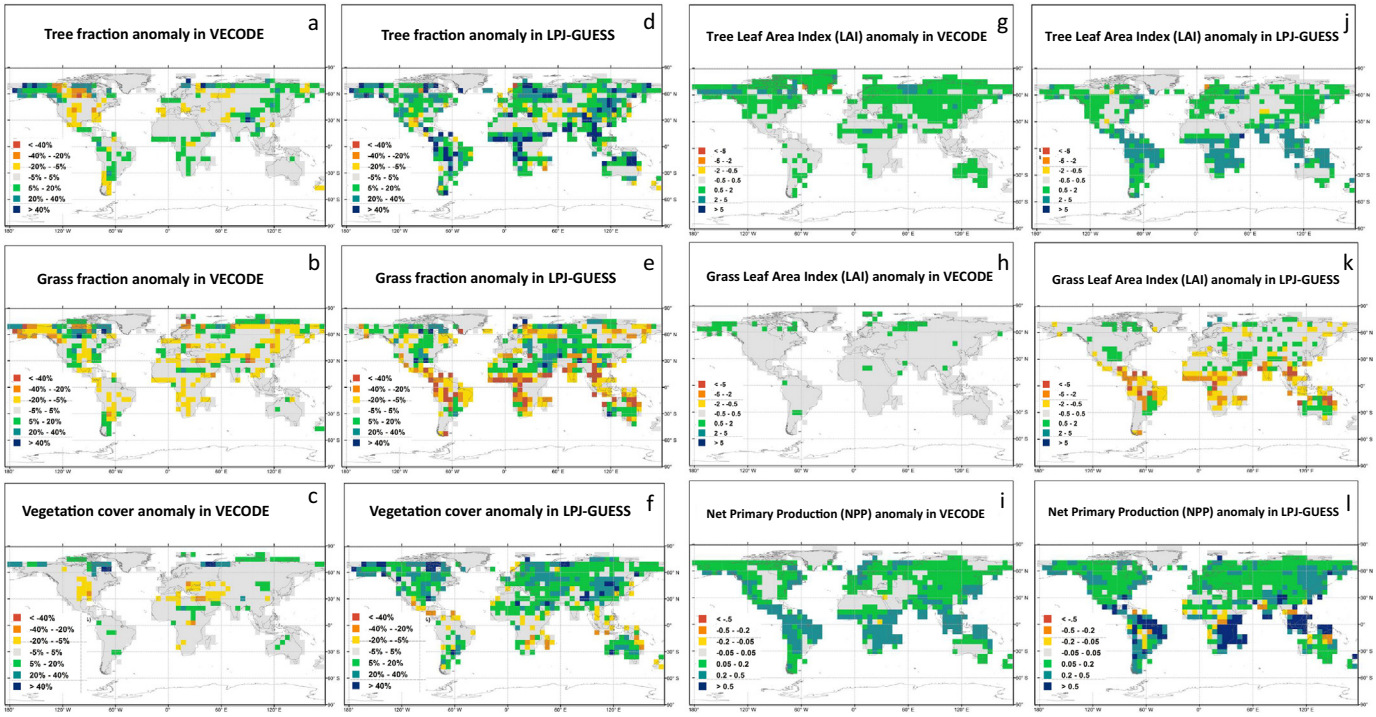

Fig. 5. Changes in vegetation coverage (%) and LAI (m^2/m^2) for aggregated PFTs, total vegetation cover and NPP (kgC/yr/m^2) under climate change (FIX0K_2CO_2-FIX0K) in VECODE (FIX0K_2CO_2-VEC and FIX0K-VEC) and LPJ-GUESS (FIX0K_2CO_2-LPJ and FIX0K-LPJ).

produce enhanced vegetation cover under FIX0K_2CO_2 (Fig. 5a–f) and FIX0K_4CO_2 (Fig. 6a-6f) conditions, including higher tree and grass cover (Fig. 5a–f) in the Northern Hemisphere and most tree cover rises at the expense of grass cover in the Southern Hemisphere, also with stronger vegetation responses in LPJ-GUESS than in VECODE. Under the 2*CO_2 and 4*CO_2 scenarios, LPJ-GUESS simulates 15% and > 20% rises in global tree cover, respectively. This is mainly in response to the extension of tropical forest and poleward shift of boreal forest, and strong decline (15% and 20%) in tropical grass cover; but the tree cover rises only by around 4% and 5% under these two scenarios in VECODE. Under the two higher CO_2 scenarios, the modelled poleward tree expansions are related to the replacement of tundra by taiga, in response to a warmer climate at northern high latitudes. In contrast, the simulated promotion of tropical forests is attributed to the reduced

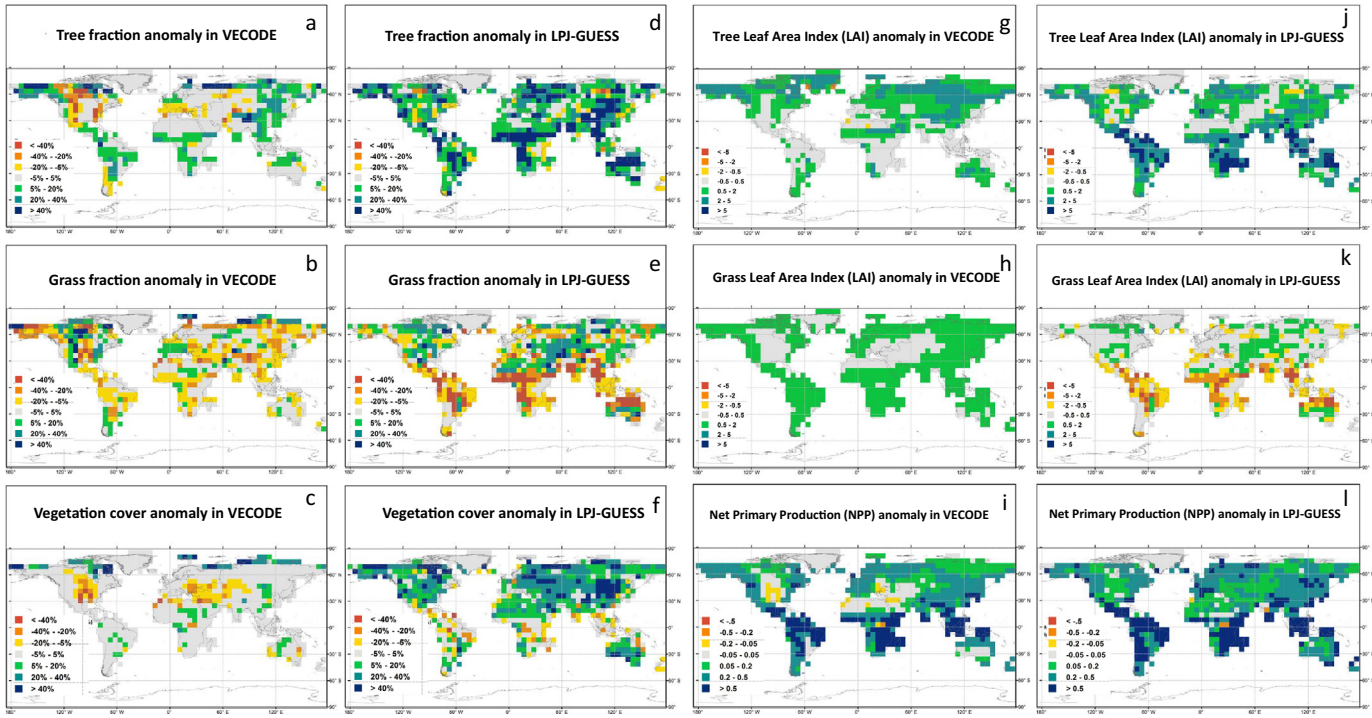

Fig. 6. Changes in vegetation coverage (%) and LAI (m^2/m^2) for aggregated PFTs, total vegetation cover and NPP (kgC/yr/m^2) under climate change (FIX0K_4CO_2-FIX0K) in VECODE (FIX0K_4CO_2-VEC and FIX0K-VEC) and LPJ-GUESS (FIX0K_4CO_2-LPJ and FIX0K-LPJ).

limitation in precipitation and the elevated CO_2 levels. The extent of complexity in eco-physiological processes in the two models mainly contributes to their marked differences in simulated tropical vegetation dynamics. LPJ-GUESS simulates up to 30% increase in tropical tree cover, in response to the quadrupled CO_2, referred to as "CO_2 fertilization", stimulating the growth of trees through the increasing rate of CO_2 reactions with rubisco during photosynthesis (Bazzaz, 1990; Long, 1991; Drake et al., 1997; Ainsworth and Long, 2005). In addition, stomatal density (Woodward and Kelly, 1995) and conductance (Medlyn et al., 2001) generally decreases with elevated CO_2, also leading to lower transpiration and more efficient water usage (Field et al., 1995; Woodward and Kelly, 1995). However, VECODE simulates only up to 5% increase under 4*CO_2 in tropical tree cover.

The changes of LAI and NPP (Figs. 5g–l and 6g–l) under higher CO_2 scenarios (FIX0K_2CO_2 and FIX0K_4CO_2) are consistent with their vegetation cover anomalies. LPJ-GUESS and VECODE simulate higher global NPP, 44% and 36%, respectively, under the 2*CO_2 scenario (warmer by 2.6 °C and elevated CO_2 by 280 ppm). These simulated increases in the two models are both higher than those simulated by five DGVMs in Sitch et al. (2008), ranging from 18% to 34%, and a median value of 23% for the forest sites in the Free-Air-CO_2 Enrichment experiments (FACE, Norby et al., 2005) when atmospheric CO_2 is elevated from ambient concentrations (370 ppmv) to 550 ppmv. However, the percentages of increases in NPP per 100 ppmv elevated CO_2 (15.7%/100 ppm in LPJ-GUESS, and 12.9%/ppm in VECODE) are in agreement with ranges (10%/100 ppm - 18.9%/100 ppm) of the five DGVMs in Sitch et al. (2008) and the results (12.8%/100 ppm) in FACE experiments (Norby et al., 2005), indicating the large impacts of CO_2 slopes on NPP. However, the underlying tropical responses of our two models and the five DGVMs in Sitch et al. (2008) are markedly different. Sitch et al. (2008) simulate Amazon dieback in response to the reduction in precipitation from 1860 to 2099 predicted by HadCM3C, but we simulate increased tropical tree cover and NPP in response to both increased simulated precipitation and elevated CO_2 from pre-industrial to 2*CO_2 scenario. Moreover, the two DGVMs in our study simulate increases in tree cover and vegetation carbon over tundra ecosystems, involving a northward shift of the tree line in response to climate warming, with longer growing seasons and elevated CO_2 levels stimulating plant production. Such poleward tree cover shifts in tundra regions are consistent with modelled results by ORCHIDEE, TRIFFID and LPJ-DGVM in Sitch et al. (2008), in agreement with observational trends in Alaska (Silapaswan et al., 2001; Sturm et al., 2001; Stow et al., 2004; Sitch et al., 2007).

3.4. *Vegetation sensitivities to climate forcing and CO_2 concentrations*

Compared with VECODE, the more mixed PFT compositions in LPJ-GUESS indicate its higher level of complexity (Fig. 7). The percentage of gridcells with clear mixtures of the three PFTs (i.e., each PFT's fraction ≥ 20%) see a rise from 4% under FIX0K_½CO_2 to 11% under FIX0K_4CO_2 in LPJ-GUESS, while it remains 0% in VECODE under all considered conditions. This linear treatment of vegetation (i.e. either forest or desert combines with grass) in VECODE suits better the classification scheme in terms of dominant PFTs than LPJ-GUESS which often includes mixed vegetation information (not shown here), and it also leads to the higher kappa coefficient in VECODE under pre-industrial conditions. In addition, most of gridcells with clear mixtures in LPJ-GUESS are distributed in vegetation transition zones, e.g., the tundra-taiga regions, implying a higher sensitivity of vegetation to climates in this more complex model. However, the two DGVMs are in agreement with change patterns in distributions of their PFTs compositions under different climate conditions, which are consistent with their simulated global vegetation (Figs. 4, 5, 6).They produce an increasing number of grid cells with high tree fraction from FIX0K_½CO_2 state (Fig. 7a), pre-industrial (Fig. 7b), FIX0K_2CO_2 state (Fig. 7c) to FIX0K_4CO_2 state (Fig. 7d), indicating coherent vegetation responses patterns to identical climate conditions although with different magnitudes.

The two DGVMs agree on sensitivity patterns to temperature (from -1.5 ($°C^{-1}$) to 1.5 ($°C^{-1}$)) (Fig. 8), in particular under climate change from mid-Holocene to pre-industrial (Fig. 8a). They simulate a similar sensitivity (about 0.15 ($°C^{-1}$)) at northern high latitudes and show

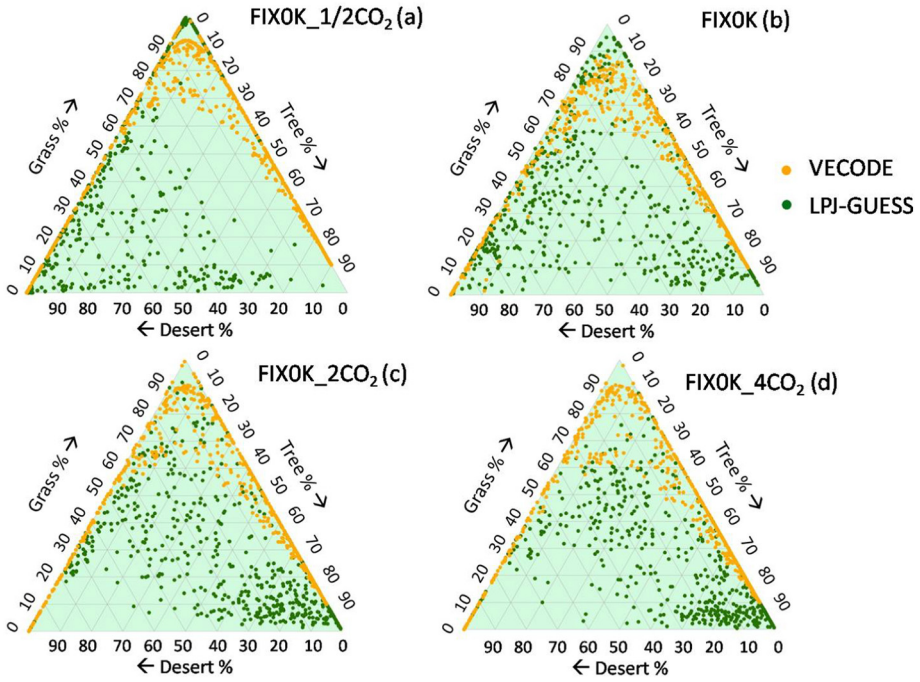

Fig. 7. Proportion of the simulated PNV cover represented by PFT-fractions in VECODE and LPJ-GUESS under four pre-industrial scenarios with different CO_2 levels (FIX0K-½CO_2, FIX0K, FIX0K-2CO_2, and FIX0K-4CO_2).

divergence in other regions between 6 ka and 0 ka (Fig. 8a), which implies a consensus on positive poleward vegetation responses to increasing temperature and also indicates more complex responses in other regions related to models' complexity. LPJ-GUESS simulates lower mid-latitude and northern tropical sensitivity (-0.25 ($^{\circ}C^{-1}$)) related to its stronger reduction in vegetation cover, whereas the slightly decreased tree cover is attributed to the smaller amplitude of VECODE sensitivity (-0.05($^{\circ}C^{-1}$)).

In addition to the two DGVMs' similar sensitivity (Fig. 8a) to climate change from 6 ka to 0 ka, the magnitude of their tropical sensitivity (Fig. 8b–d) varies markedly under CO_2 scenarios, associated with their complexity of eco-physiological processes. Under colder and dryer conditions (FIX0K_½CO_2) with lower CO_2 level, LPJ-GUESS simulates an up to 0.5 ($^{\circ}C^{-1}$) tropical sensitivity related to the large reduction in tree-cover due to the modified C3/C4 competition, whereas the sensitivity remains below 0.2 ($^{\circ}C^{-1}$) in VECODE. Several studies on the contribution of lower CO_2 to vegetation dynamics during the LGM (Prentice and Harrison, 2009; Prentice et al., 2011; Woillez et al., 2011; Claussen et al., 2013) suggested that the contraction of tropical forest cover is a predictable outcome of the low CO_2 concentration. The large extension of tropical grass in LPJ-GUESS is at the expense of trees in response to the effect of lower CO_2 on C3-plant photosynthesis and the higher ability of carboxylation in C4 plants (Gerber et al., 2004), indicating the key function of lower CO_2 concentration in tropical vegetation. In contrast, this is hardly detected by VECODE due to its independence of vegetation-cover on varying CO_2 and the climate-dependent ecophysiological processes. Also, LPJ-GUESS simulates about 0.25 ($^{\circ}C^{-1}$) tropical sensitivity under the 2*CO_2 scenario (Fig. 8c) and 0.15 ($^{\circ}C^{-1}$) under the 4*CO_2 scenario (Fig. 8d), while it remains around 0 ($^{\circ}C^{-1}$) in VECODE. The decreased sensitivities with the elevated CO_2 concentrations, in particular in LPJ-GUESS, are related to the limited availability of Nitrogen (Hungate et al., 2003; Luo et al., 2004).

In order to isolate the impacts of climate forcing and CO_2 levels on tropical vegetation which involves large divergences between the two models, we plot how tropical (20°S–20°N) tree-cover changes with CO_2 concentration and rainfall in the two DGVMs (Fig. 9). Under identical CO_2 concentrations (280 ppm), the two models simulate a dominance (tree cover ≥ 0.5) of tropical trees (Fig. 9a, b) at sites with rainfall higher than about 1500 mm under pre-industrial conditions (FIX0K),

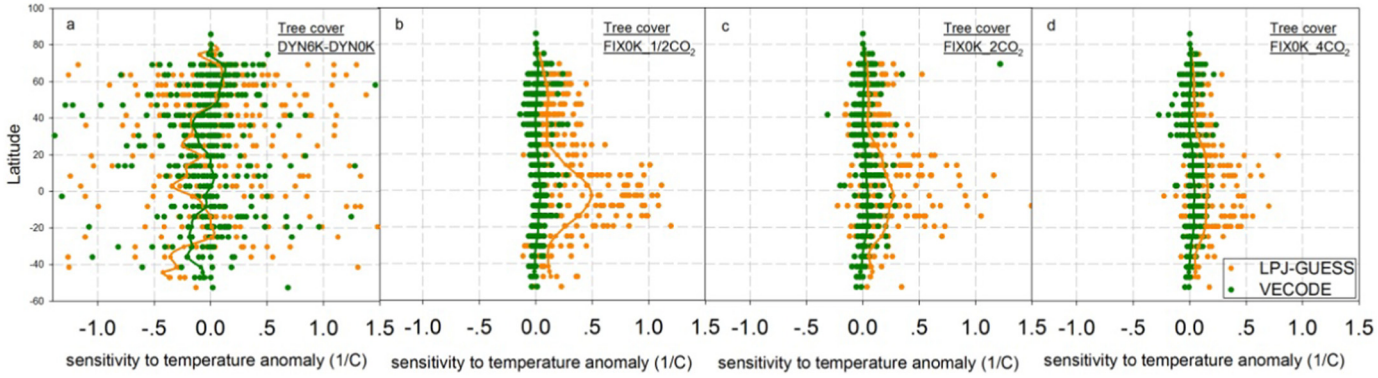

Fig. 8. Latitudinal sensitivity of tree cover in the two models to temperature anomalies between DYN6K and DYN0K (a), FIX0K_½CO_2 and FIX0K (b), FIX0K_2CO_2 and FIX0K (c), FIX0K_4CO_2 and FIX0K (d).

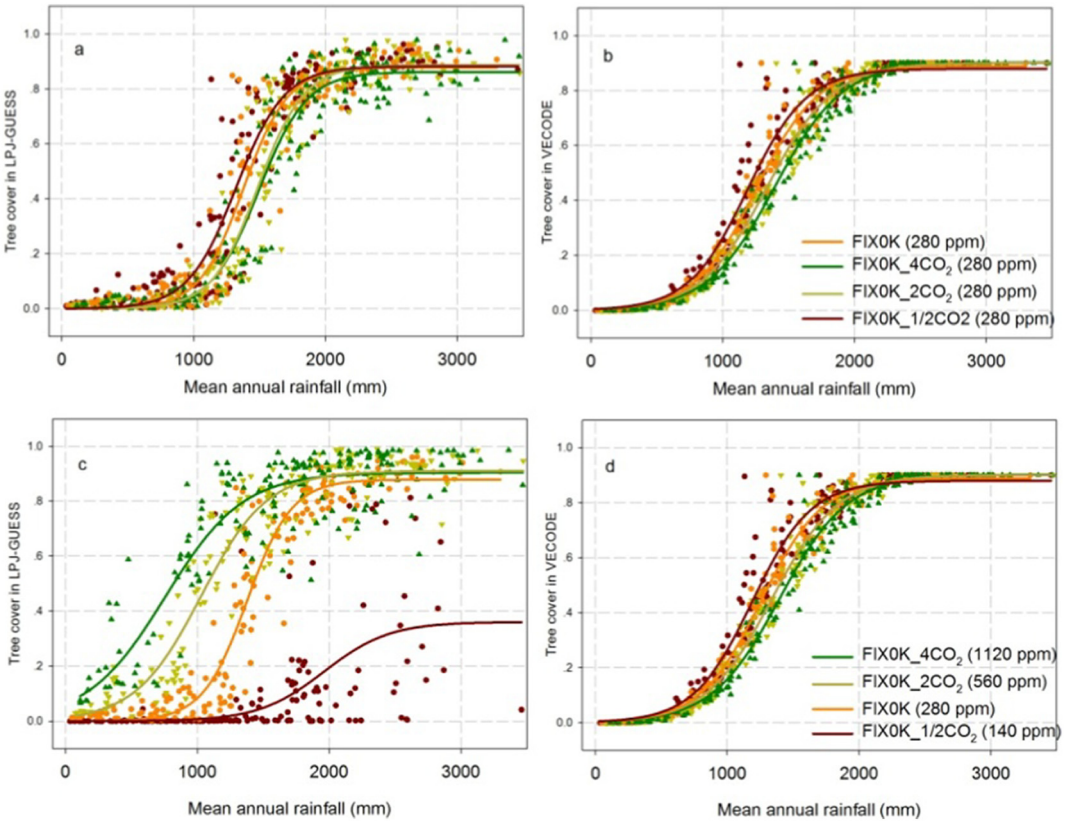

Fig. 9. Sensitivity of tropical tree-cover in the two DGVMs to rainfall and atmospheric CO_2 concentrations. The simulated tropical tree cover in LPJ-GUESS (a) and VECODE (b) as a function of rainfall under different climate states with identical CO_2 concentration (280 ppm); and the tropical tree cover in LPJ-GUESS (c) and VECODE (d) as a function of rainfall under different climate states with varying CO_2 concentration.

and it requires about 1400 mm and 1600 mm rainfall under colder (½*CO_2 scenario) and warmer (4*CO_2 scenario) conditions, respectively. This indicates a slightly smaller rainfall requirement under colder conditions related to reduced evaporation. In contrast, the requirements of rainfall for dominant tropical cover experience marked changes when accounting for variations in CO_2 concentrations (Fig. 9c, d). Under the 4*CO_2 scenario, only about 800 mm rainfall is required by tropical trees dominant sites in LPJ-GUESS, as a result of the increased water use efficiency due to the decreased stomatal density and conductance with rising atmospheric CO_2 concentrations (Field et al., 1995; Woodward and Kelly, 1995; Drake et al., 1997). In contrast, tropical trees (Fig. 9c) do not really become dominant under halved CO_2 concentration condition due to evolvement and spread of C4 plants that are more competitive relative to C3 plants at low CO_2 (Cole and Monger, 1994; Ehleringer et al., 1997; Collatz et al., 1998). The modelled impacts of varying CO_2 on tropical trees are consistent with the sensitivity of African C3/C4-plants to rainfall and CO_2 concentrations simulated by aDGVM (Higgins and Scheiter, 2012). Moreover, the requirement of rainfall decreases nonlinearly with elevated CO_2 concentrations (Fig. 9c), implying a decline in vegetation sensitivity to CO_2 levels, which might be related to the limited availability of Nitrogen (Hungate et al., 2003; Luo et al., 2004). In contrast, these impacts of varying CO_2 on tropical trees are not detected by VECODE (Fig. 9d) due to its independence of PFT cover from CO_2 concentration, but they are somewhat reflected by the responses of tropical tree-LAI to rainfall and CO_2 concentration (Fig. 10b, d), although these impacts are much weaker compared to LPJ-GUESS (Fig. 10a, c).

4. Discussion: implications and outlook

Based on the modelled vegetation in the two models under different climate and CO_2 change states, we answer in this section the following three questions raised in Section 1: 1) are the two DGVMs able to simulate pre-industrial vegetation dynamics; 2) how sensitive are the vegetation dynamics in the two DGVMs to climate and atmospheric CO_2 changes; and 3) what are the relative uncertainties in simulating vegetation dynamics and functions associated with different choices of DGVMs?

4.1. The pre-industrial potential natural vegetation distribution

Our results show that the two DGVMs produce consistent pre-industrial natural vegetation distributions, and they are generally in agreement with independent global gridded PNV (Levavasseur et al., 2012), but they agree much less (differs by 20%) in the way they simulate the desert distribution. We assign the simulated abundances of the PFTs to two dominant PFTs groups in line with VECODE to compare the modelled pre-industrial vegetation in the two models, using the simple classification scheme explained in Table 2.

In our study, the modelled pre-industrial vegetation is described by composition of 11 and 2 PFTs in LPJ-GUESS and VECODE, respectively, and our reference PNV-dataset (Levavasseur et al., 2012) includes 10 biomes. According to the decision of defined vegetation types in previous studies, we can combine the compositions of PFTs in the two models to 10 biomes to keep in line with the reference PNV dataset. However, the composition of 2 PFTs in VECODE does not separate different tree types or distinguish stand heights of PFTs, indicating the unsuitability for using the FPC-based scheme in Schurgers et al. (2006) or the scheme combined with stand height (Joos et al., 2004). Besides, the LAI scheme (Hickler et al., 2006) is also not suitable for VECODE due to its overestimation in tree LAI (seen in to 3.4). As a result, our FPC-based scheme for two determined vegetation types avoids the uncertainties related to LAI and upscaling for VECODE, but this scheme buffers detailed vegetation dynamics during the downscaling processes

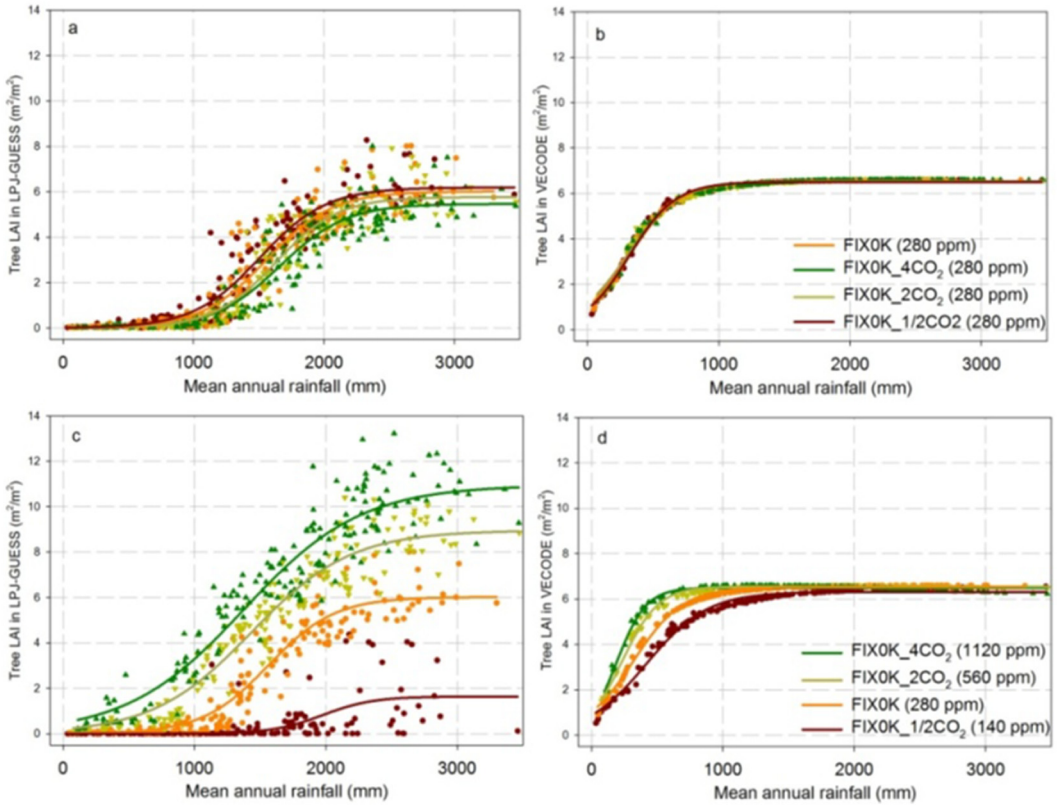

Fig. 10. Sensitivity of tropical tree-LAI in the two DGVMs to rainfall and atmospheric CO_2 concentrations. The simulated tropical tree-LAI in LPJ-GUESS (a) and VECODE (b) as a function of rainfall under different climate states with identical CO_2 concentration (280 ppm); and the tropical tree-LAI in LPJ-GUESS (c) and VECODE (d) as a function of rainfall under different climate states with varying CO_2 concentration.

in LPJ-GUESS, e.g., combining tree-PFTs (boreal, temperate and tropical trees) together. These buffers are largely attributed to the mixed composition of three PFTs in LPJ-GUESS (Fig. 7) since most of gridcells with clear mixtures are distributed in vegetation transition zones, e.g., the tundra-taiga regions and the forest-savanna-grass regions.

We conclude that our classification scheme is a useful approach to produce modelled PNV in multiple models, and the combination of kappa statistics and matching ratios allow for quantitative comparisons among multiple models and data. This approach captures tree distributions in the two models well, with the highest matching ratio of trees (about 80%). However, as mentioned at the start of Section 3.1, the downscaling of PFTs in a more complex DGVM (LPJ-GUESS) failed to distinguish accurately between grass and desert, involving a larger extent of grass in the tropics, contributing to its lower kappa coefficient. As a result, for comparison purposes, we conclude that our approach of downscaling PFTs for more complex DGVMs is suitable for tree distributions, but people should be cautious using this approach when comparing in detail grass and desert cover in multiple models. Moreover, comparisons among multiple DGVMs are widely discussed in vegetation studies, but they often applied different sets of defined vegetation types, which increase the difficulties in interpretation of the comparisons. Thus, to summarize, the combination of the downscaling approach and a standard set of vegetation types (e.g., Dallmeyer et al., 2019) will be useful to future studies.

Table 2
Assignment of dominant PFTs as the VECODE output.

VECODE-PFTs	LPJ-GUESS-PFTs	PNV in Levavasseur et al., 2012
Tree	Boreal needle-leaved evergreen trees	Boreal forest
		Temperate forest
	Boreal needle-leaved evergreen shade-intolerant trees	Tropical forest
	Boreal needle-leaved summer-green trees	Warm-temperate forest
	Temperate broadleaved summer-green trees	
	Boreal-temperate broadleaved summer-green trees	
	Temperate broadleaved evergreen trees	
	Tropical broadleaved evergreen trees	
	Tropical broadleaved evergreen shade-intolerant trees	
	Temperate broadleaved raingreen trees	
Grass	C3-grass, C4-grass	Desert-vegetation
		Grassland
		Savanna
		Tundra
Desert	Other	Warm-desert
		Cold-desert

4.2. Vegetation sensitivities to climate and CO_2 concentration

Both DGVMs capture decreased slopes of global LAI with increasing atmospheric CO_2 from pre-industrial level to 4*CO_2 scenario, indicating a reduction in LAI sensitivity to elevated CO_2, related to the expected saturation of the direct CO_2 physiological fertilizing effect at high CO_2 concentrations (Cao and Woodward, 1998). The modelled relative rises in global mean LAI due to CO_2 fertilization alone is about 15% (or 5% per 100 ppm) in LPJ-GUESS and it is about 9% (or 3% per 100 ppm) in VECODE from pre-industrial condition (280 ppm) to 560 ppm under 2*CO_2 scenario, which is comparable to measurements from the Free-Air-CO_2 Enrichment experiments (0.3–11.1%, or 0.6–24.1% per 100 ppm) from present condition (370 ppm) to 550 ppm (Norby et al., 2005). Moreover, from pre-industrial conditions to 4*CO_2 scenario, the modelled total LAI increase is about 34% (or 4% per 100 ppm) in LPJ-GUESS and it is about 15% (or 2% per 100 ppm) in VECODE. Similar to the LAI responses to elevated CO_2 in the two models, the impacts of CO_2 fertilization alone on the global NPP also decrease, including 7% and 5% increase per 100 ppm from pre-industrial to 2*CO_2 and 4*CO_2 scenario in LPJ-GUESS, and 5% and 3% increase per 100 ppm from pre-industrial to 2*CO_2 and 4*CO_2 scenario in VECODE.

The global trend towards increased vegetation cover (Fig. 11a), LAI (Fig. 11b) and total NPP (Fig. 11c) is attributed to different regional responses with the varying CO_2 concentrations (from ½*CO_2 to 4*CO_2 level). It is a function of the conditions under which CO_2 level shifts the competitive balance in favor of grasses or trees, in particular in tropical regions (Fig. 11j–l), but this function is weaker at northern high latitudes, where the temperature is dominant factor shaping vegetation change (Seddon et al., 2016). Although the two models in our study simulate consistent increases in LAI and total NPP with five DGVMs in Sitch et al. (2008), their responses are highly related to the complexity. LPJ-GUESS simulates the shifted competitive balance between tree and grass under lower and higher CO_2 levels, but VECODE hardly captures them.

The similar increased LAI in VECODE to LPJ-GUESS, in particular under higher CO_2 levels, is a result of LAI overestimation in VECODE and also of the dependence on modelled climate changes which are not identical with Sitch et al. (2008). Moreover, the impacts of CO_2 levels on vegetation vary with climate conditions, but the sensitivities of DGVMs with consideration of the dependence of CO_2 effects on climate conditions have never been compared in a systematic way. Therefore, these should be detected by forcing multiple DGVMs with the same set of climate and CO_2 change scenarios so that the ranges of vegetation sensitivities to climate and varying can be determined systematically.

4.3. The uncertainties related to model complexity

One source of uncertainty is related to the aggregated vegetation types from PFTs in the two models and their different complexity. We aggregated the PFTs to tree and grass for comparison purposes, merging more detailed vegetation responses to some extent, which might induce an underestimation in sensitivity. In addition, although both models simulate coherent patterns of vegetation dynamics in response to different climate states, magnitudes are markedly different mainly due to their different sensitivity to varying CO_2 levels. Moreover, a positive feedback loop (refer to 3.4) works in LPJ-GUESS related to its sensitivity to CO_2 levels, which is consistent with simulated vegetation responses by aDGVM in Africa (Higgins and Scheiter, 2012). As a result, their marked differences imply not only the different complexity of ecophysiological processes, but also the complexity-induced differences in requirements of climatic factors, e.g., the requirement of rainfall for tropical forest. However, the range of the DGVM sensitivity and to what extent it affects vegetation simulation with varying CO_2 still needs to be performed by involving more DGVMs with different complexity, and more detail vegetation types might help the detection for impacts of sensitivity.

A second major source of uncertainty is related to the omission of potentially important processes during our vegetation simulations:

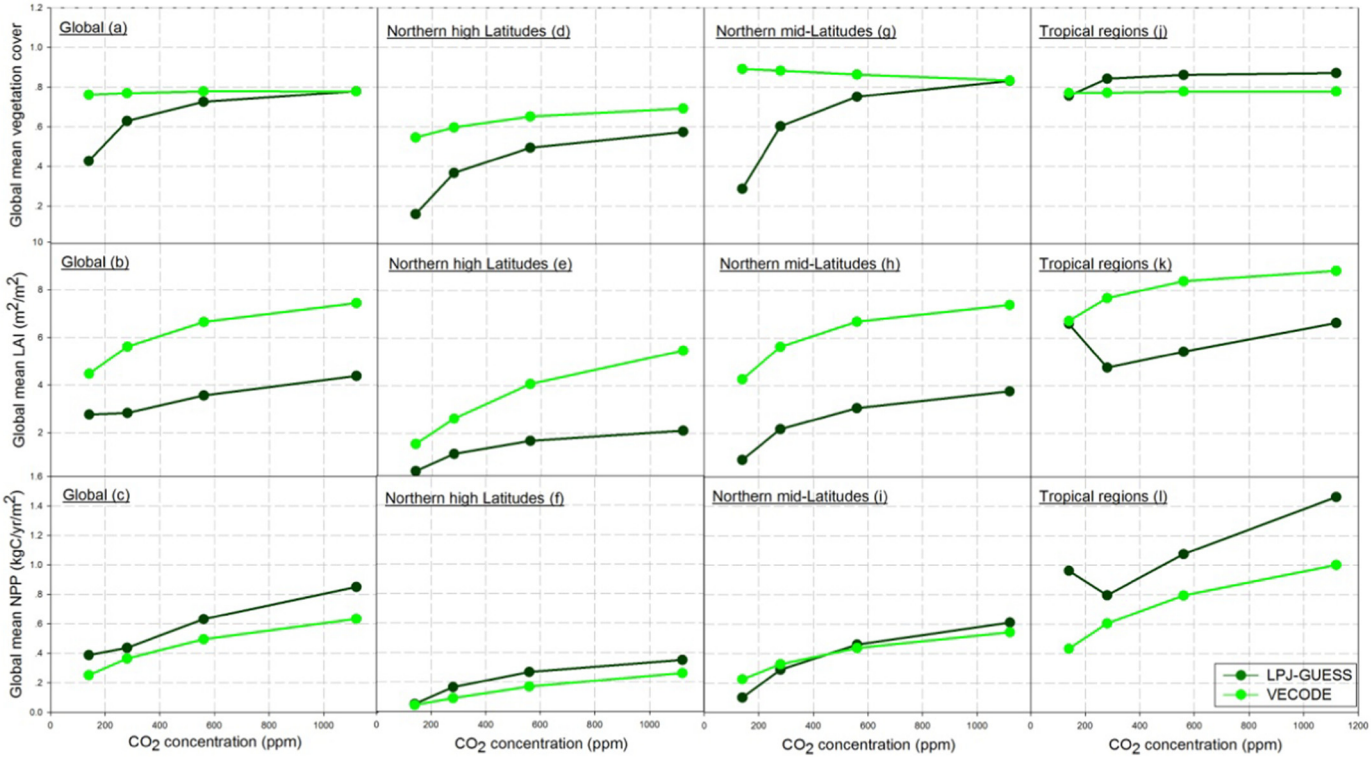

Fig. 11. Comparisons of the simulated Global vegetation cover, LAI and NPP (a, b, c); Northern high latitudinal vegetation cover, LAI and NPP (d, e, f); Northern mid-latitudinal vegetation cover, LAI and NPP (g, h, i); and Tropical vegetation cover, LAI and NPP (j, k, l) in the two DGVMs under four scenarios with different CO_2 levels (FIX0K-½CO_2, FIX0K, FIX0K-2CO_2, and FIX0K-4CO_2).

terrestrial climate-carbon feedbacks and nitrogen limitation. The implication of the exclusion of these processes is discussed next.

Positive terrestrial climate-carbon cycle feedbacks accelerate the rate of CO_2 increase via the response of land carbon cycle to climate change in different 21st Century greenhouse gas emission scenario runs (Sitch et al., 2008), but magnitude of this acceleration is highly dependent on choice of DGVMs. The main contribution of this difference is DGVMs' different reductions in tropical NPP and decreases in extratropical soil residence time (Sitch et al., 2008). As a result, we might underestimate the impacts of elevated CO_2 due to the disregarded positive feedbacks and our two models' potential differences in simulating feedbacks. Also, how the regional factors impact on the climate-carbon cycle feedback still needs to be studied by doing sensitivity experiments with multiple DGVMs. In addition, the dependence of this feedback on climate conditions should also be taken into account in further studies.

The C–N interactions play important roles on land carbon storage, Hungate et al. (2003) estimated upper and lower limits for possible future N supply and compared these with the increased requirement by vegetation (Cramer et al., 2001), suggesting an overestimation in potential increase in ecosystem carbon storage, especially the fertilization effect of elevated CO_2 levels. In addition, Zaehle and Dalmonech (2011) pointed out that nitrogen cycling leads to an acceleration of atmospheric carbon accumulation through reductions in both global carbon sequestration and the carbon storages with increasing CO_2 levels. Moreover, Smith et al. (2014) simulated the implications of accounting for C-N interactions on predictions of LPJ-GUESS relative to C-cycle only simulations, including improved simulation for broadleaved forests. They also highlight the dependence of N limitation on climate conditions: N limitation reduces productivity of cold- and dry-climate ecosystem relative to mesic temperate and tropical ecosystems, also, it reduces CO_2 enhancement of NPP for boreal forest. In our study, the vegetation responses to the elevated CO_2, in particular the $4*CO_2$ condition, might also include overestimations in carbon storage due to the C-only simulations. Therefore, the functions of carbon-nitrogen interactions on land carbon cycle still need to be understood in future, during which the dependence of N limitation on climate conditions should also be taken into account.

5. Conclusions

In our study, we simulate vegetation dynamics in two DGVMs under observed pre-industrial climate and four climate change scenarios, including past climate changes (from mid-Holocene to pre-industrial) and scenarios with halved, doubled and quadrupled CO_2 concentration (140 ppm, 560 ppm, and 1120 ppm).The two models are consistent with pre-industrial vegetation dynamics, involving 67% and 61% agreement with independent global gridded PNV (Levavasseur et al., 2012) in VECODE and LPJ-GUESS, respectively. They capture vegetation increase between 6 ka and 0 ka in Northern Africa, the Middle East, and northern high latitudes in response to the climate change. Also, they simulate enhanced vegetation in response to warming climate and increasing CO_2 concentration. However, the magnitudes of vegetation responses under all CO_2 scenarios vary markedly between the two DGVMs, including about 20% and 3% reduction in global tree-cover in LPJ-GUESS and VECODE under lower CO_2 scenario; about 15% and 4% increase under $2*CO_2$ scenario; and about 20% and 5% increase under $4*CO_2$ scenario. On the basis of the results we conclude the following.

1. The better agreement of VECODE with independent PNV (Levavasseur et al., 2012) is attributed to its more linear PFTs' composition, which suits better to the classification scheme in terms of dominant PFTs than LPJ-GUESS which often includes mixed vegetation information. The models' complexity impacts on vegetation sensitivity to temperature slightly when the atmospheric CO_2 level varies slight compared to pre-industrial level (280 ppm), indicated by the two DGVMs' agreement on their simulations between Mid-Holocene and pre-industrial.
2. The complexity of the two DGVMs largely impacts on vegetation sensitivity to CO_2 concentrations, implying the significant importance of ecophysiological effects. LPJ-GUESS and VECODE simulate declines in global NPP about 11% and 31% under $½*CO_2$ scenario, respectively. Compared with the LGM, the less reduction in LPJ-GUESS is related to the larger extension of tropical grass due to the more competitive C4 plants under warmer condition with lower CO_2 concentration, but the comparable value in VECODE is related to its climate-dependent competition. Likewise, the complexity of eco-physiological processes also plays an important role on vegetation responses under elevated CO_2 states. LPJ-GUESS simulates a 44% increase in global NPP from FIX0K to $2*CO_2$ scenario compared to 36% in VECODE, in response to the warmer and elevated CO_2. Physiological effects do scale up to ecosystem effects, through changes in primary production and through competition between plants with different photosynthetic pathways.
3. The complexity also plays roles on the vegetation requirements of climatic factors due to the physiological effects that more efficient water use of vegetation is facilitated under elevated atmospheric CO_2 concentration. In LPJ-GUESS, dominant distribution of tropical trees requires only around 800 mm rainfall under the $4*CO_2$scenario, much less than (about 1500 mm) under pre-industrial forcing. Yet, tropical trees hardly become dominant under $½*CO_2$ scenario whatever the amount of rainfall is due to the development of more competitive C4 plants. However, these complexity-induced impacts are not significantly simulated in VECODE due to its independence of PFT fraction to atmospheric CO_2 levels and overestimation in tree LAI.
4. Comparisons among multiple DGVMs are widely used in vegetation studies but they are often among different sets of vegetation types, thus a standard set of vegetation types benefits for comparison purposes in future studies. The uncertainties in DGVMs are highly related to the inclusion of ecosystem processes and the scale of vegetation classification. Also, future challenges are the systematic simulations of the vegetation sensitivity to varying $CO_2$and climate by forcing multiple DGVMs with identical sets of climate and CO_2 change scenarios. During these studies, the impact of regional contributions (mainly including the responses of tropical NPP and extratropical soil residence time) on the climate-carbon cycle feedback should be taken into account. Moreover, the impacts of N limitation on vegetation and its dependence on climate are needed to be accounted for.

Acknowledgements

We sincerely thank Victor Brovkin for valuable comments and suggestions. We would also thank the LPJ-GUESS team for making their model available for our research. This work was supported by the China Scholarship Council (201506180059).

Appendix A. Supplementary data

Supplementary data to this article can be found online at https://doi.org/10.1016/j.gloplacha.2019.05.009.

References

Ainsworth, E.A., Long, S.P., 2005. What have we learned from 15 years of free-air CO_2 enrichment (FACE)? A meta-analytic review of the responses of photosynthesis, canopy properties and plant production to rising CO_2. New Phytol. 165 (2), 351–372.
Arora, V.K., 2002. Modeling vegetation as a dynamic component in soil–vegetation–atmosphere transfer schemes and hydrological models. Rev. Geophys. 40 (2), 3-1–3-26.
Badeck, F.W., Bondeau, A., Böttcher, K., Doktor, D., Lucht, W., Schaber, J., Sitch, S., 2004. Responses of spring phenology to climate change. NewPhytol 162, 295–309.
Bazzaz, F.A., 1990. The response of natural ecosystems to the rising global CO_2 levels. Annu. Rev. Ecol. Syst. 21, 167–196.

Bonan, G.B., 2008. Forests and climate change: forcing, feedbacks, and the climate benefits of forests. Science 320, 1444–1449.
Bond, W.J., Midgely, G.F., Woodward, F.I., 2003. The importance of low CO_2 and fire in promoting the spread of grasslands and savannas. Glob. Chang. Biol. 9, 973–982.
Brovkin, V., Ganopolski, A., Svirezhev, Y., 1997. A continuous climate-vegetation classification for use in climate-biosphere studies. Ecol. Model. 101, 251–261.
Brovkin, V., Bendtsen, J., Claussen, M., Ganopolski, A., Kubatzki, C., Petoukhov, V., Andreev, A., 2002. Carbon cycle, vegetation, and climate dynamics in the Holocene: experiments with the CLIMBER-2 model. Global Biogeochem. Cy. 16 (1139), 1113–1131.
Brovkin, V., Raddatz, T., Reick, C., Claussen, M., Gayler, V., 2009. Global biogeophysical interaction between forest and climate. Geophys. Res. Lett. 36, L07405.
Calvo, M.M., Prentice, I.C., 2015. Effects of fire and CO_2 on biogeography and primary production in glacial and modern climates. New Phytol. 208, 987–994.
Cao, M., Woodward, F.I., 1998. Net primary and eco-system production and carbon stocks of terrestrial ecosys-tems and their responses to climate change. Glob. Chang. Biol. 4, 185–198.
Ciais, P., Dolman, A.J., Bombelli, A., Duren, R., Peregon, A., Rayner, P.J., Miller, C., Gobron, N., Kinderman, G., Marland, G., Gruber, N., Chevallier, F., Andres, R.J., Balsamo, G., Bopp, L., Breon, F.M., Broquet, G., Dargaville, R., Battin, T.J., Borges, A., Bovensmann, H., Bruchwitz, M., Butler, J., Claussen, M., Gayler, V., 1997. The greening of the Sahara during the mid-Holocene: results of an interactive atmosphere-biomemodel. Global Ecol. Biogeogr.Lett. 6 (5), 369–377.
Claussen, M., Gayler, V., 1997. The greening of the Sahara during the mid-Holocene: results of an interactive atmosphere-biome model. Glob. Ecol. Biogeogr. 6, 369–377.
Claussen, M., Selent, K., Brovkin, V., Raddatz, T., Gayler, V., 2013. Impact of CO_2 and climate on last Glacial Maximum vegetation- a factor of separation. Biogeosciences 10, 3593–3604.
Cole, D.R., Monger, H.C., 1994. Influence of atmospheric CO_2 on the decline of C4 plants during the last deglaciation. Nature 368, 533–536.
Collatz, G.J., Berry, J.A., Clark, J.S., 1998. Effects of climate and atmospheric CO_2 partial pressure on the global distribution of C4 grasses: present, past, and future. Oecologia 114, 441–454.
Cowling, S.A., Shin, Y., 2006. Simulated ecosystem threshold responses to co-varying temperature, precipitation and atmospheric CO_2 within a region of Amazonia. Glob. Ecol. Biogeogr. 15, 553–566.
Cowling, S.A., Sykes, M.T., 1999. Physiological significance of low atmospheric CO2 for plant–climate interactions. Quat. Res. 242, 237–242.
Cowling, S.A., Maslin, M.A., Sykes, M.T., 2001. Paleovegetation simulations of lowland Amazonia and implications for theories of neotropical allopatry and speciation. Quat. Res. 55, 140–149.
Cox, P., 2001. Description on the "TRIFFID" Dynamic Global Vegetation Model. Hadley Centre Technical Report 24, Met Office, Bracknell, Berkshire, UK.
Cramer, W., 1997. Using plant functional types in a global vegetation model. In: Smith, T.M. (Ed.), Plant Functional Types: Their Relevance to Ecosystem Properties and Global Change. Cambridge University Press, Cambridge, pp. 271–288.
Cramer, W., Bondeau, A., Woodward, F.I., Prentice, I.C., Betts, R.A., Brovkin, V., Cox, P.M., Fisher, V., Foley, J.A., Friend, A.D., Kucharik, C., Lomas, M.R., Pamankutty, N., Stich, S., Smith, B., White, A., Young-molling, C., 2001. Global response of terrestrial ecosystem structure and function to CO_2 and climate change: results from six dynamic global vegetation models. Glob. Chang. Biol. 7, 357–373.
Crucifix, M., Loutre, M.F., Tulkens, P., Fichefet, T., Berger, A., 2002. Climate evolution during the Holocene: a study with an Earth system model of intermediate complexity. Clim. Dyn. 19, 43–60.
Dallmeyer, A., Claussen, M., Otto, J., 2010. Contribution of oceanic and vegetation feedbacks to Holocene climate change in monsoonal Asia. Clim. Past 6, 195–218.
Dallmeyer, A., Claussen, M., Brovkin, V., 2019. Harmonising plant functional type distributions for evaluating Earth system models. Clim. Past 15 (1), 335–366.
den Elzen, M., Beusen, A., Rothmans, J., 1995. Modelling Global Biogeochemical Cycles: An Integrated Assessment Approach, Natural Institute of Public Health and the Environment (RIVM). (Bilthoven).
Denman, K.L., Brasseur, G., Chidthaisong, A., Ciais, P., Cox, P.M., Dickinson, R.E., Hauglustaine, D., Heinze, C., Holland, E., Jacob, D., Lohmann, U., Ramachandran, S., da Silva Dias, P.L., Wofsy, S.C., Zhang, X., 2007. Couplings between changes in the climate system and biogeochemistry. Climate Change 2007: The Physical Science Basis. In: Contribution of Working Group I to the Fourth Assessment Report of the Intergovernmental Panel on Climate Change, pp. 500–587.
Drake, B.G., Gonzales-Meler, M.A., Long, S.P., 1997. More efficient plants: a consequence of rising atmospheric CO_2? Annu. Rev. Plant Physiol. Plant Mol. Biol. 48, 609–639.
Ehleringer, J.R., Cerling, T.E., Helliker, B.R., 1997. C4 photosynthesis, atmospheric CO_2 and climate. Oecologia 112, 285–299.
Field, C.B., Jackson, R.B., Mooney, H.A., 1995. Stomatal responses to increased CO_2: Implications from the plant to the global scale. Plant Cell Environ. 16, 1214–1225.
Friedlingstein, P., Prentice, I.C., 2010. Carbon–climate feedbacks: a review of model and observation based estimates. Curr. Opin. Environ. Sustain. 2, 251–257.
Friedlingstein, P., Cox Betts, R., Bopp, L., Von Bloh, W., Brovkin, V., Cadule, P., Doney, S., Eby, M., Fung, I., Bala, G., Jones, C., Joos, F., Kato, T., Kawamiya, M., Knorr, W., Lindsay, K., Matthews, H.D., Raddatz, T., Rayner, P., Reick, C., Roeckner, E., Schnitzler, K.G., Schnur, R., Strassmann, K., Weaver, A.J., Yoshikawa, C., Zeng, N., 2006. Climate–carbon cycle feedback analysis: results from the C4MIP model intercomparison. J. Clim. 19, 3337–3353.
Friedlingstein, P., Meinshausen, M., Arora, V.K., Jones, C.D., Anav, A., Liddicoat, S.K., Knutti, R., 2014. Uncertainties in CMIP5 climate projections due to carbon cycle feedbacks. J. Clim. 27, 511–526.
Friend, A.D., Lucht, W., Rademacher, T.T., Keribin, R., Betts, R., Cadule, P., Ciais, P., Clark, D.B., Dankers, R., Falloon, P.D., Ito, A., Kahana, R., Kleidon, A., Lomas, M.R., Nishina, K., Ostberg, S., Pavlick, R., Peylin, P., Schaphoff, S., Vuichard, N., Warszawski, L., Wiltshire, A., Woodward, F.I., 2014. Carbon residence time dominates uncertainty in terrestrial vegetation responses to future climate and atmospheric CO_2. Proc. Natl. Acad. Sci. U. S. A. 111 (9), 3280–3285.
Furley, P.A., Proctor, J., Ratter, J.A., 1992. The Nature and Dynamics of Forest–Savannah Boundaries. Chapman and Hall, London, UK.
Galbraith, D., Levy, P.E., Sitch, S., Huntingford, C., Cox, P., Williams, M., Meir, P., 2010. Multiple mechanisms of Amazonian forest biomass losses in three dynamic global vegetation models under climate change. New Phytol. 187 (3), 647–665.
Gallimore, R., Jacob, R., Kutzbach, J., 2005. Coupled atmosphere–ocean–vegetation simulations for modern and mid-Holocene climates: role of extratropical vegetation cover feedbacks. Clim. Dyn. 25, 755–776.
Ganopolski, A., Petoukhov, V., Rahmstorf, S., Brovkin, V., Claussen, M., Eliseev, A., Kubatzki, C., 2001. CLIMBER-2: a climate system model of intermediate complexity, Part II: Model sensitivity. Clim. Dyn. 17, 735–751.
Gerber, S., Joos, F., Prentice, I.C., 2004. Sensitivity of a dynamic global vegetation model to climate and atmospheric CO_2. Glob. Chang. Biol. 10, 1223–1239.
Goosse, H., Brovkin, V., Fichefet, T., Haarsma, R., Huybrechts, P., Jongma, J., Mouchet, A., Selten, F., Barriat, P.Y., Campin, J.M., Deleersnijder, E., Driesschaert, E., Goelzer, H., Janssens, I., Loutre, M.F., Morales Maqueda, M.A., Opsteegh, T., Mathieu, P.P., Munhoven, G., Pettersson, E.J., Renssen, H., Roche, D.M., Schaeffer, M., Tartinville, B., Timmermann, A., Weber, S.L., 2010. Description of the Earth system model of intermediate complexity LOVECLIM version 1.2. Geosci. Model Dev. 3, 603–633.
Harding, R.J., Pomeroy, J.W., 1996. The energy balance of the winter boreal landscape. J. Clim. 9, 2778–2787.
Haxeltine, A., Prentice, I.C., 1996. BIOME3: an equilibrium terrestrial biosphere model based on ecophysiological constraints, resource availability, and competition among plant functional types. Global Biochem. Cy. 10, 693–709.
Hedstrom, N.R., Pomeroy, J.W., 1998. Measurements and modeling of snow interception in the boreal forest. Hydrol. Process. 12, 1611–1625.
Hickler, T., Prentice, I.C., Smith, B., Sykes, M.T., Zaehle, S., 2006. Implementing plant hydraulic architecture within the LPJ Dynamic Global Vegetation Model. Glob. Ecol. Biogeogr. 15, 567–577.
Hickler, T., Smith, B., Prentice, I.C., Mjofors, K., Miller, P., Arneth, A., Sykes, M.T., 2008. CO_2 fertilization in temperate FACE experiments not representative of boreal and tropical forests. Glob. Chang. Biol. 14, 1531–1542.
Higgins, S.I., Scheiter, S., 2012. Atmospheric CO_2 forces abrupt vegetation shifts locally, but not globally. Nature 488, 209–212.
Hughes, J.K., Valdes, P.J., Betts, R., 2006. Dynamics of a global-scale vegetation model. Ecol. Model. 198 (3–4), 452–462.
Hungate, B., Dukes, J.S., Shaw, M.R., Luo, Y., Field, C.B., 2003. Nitrogen and climate change. Science 302, 1512–1513.
IPCC, 2014. Contribution of working groups I, II and III to the fifth assessment report of the intergovernmental panel on climate change. In: Climate Change 2014: Synthesis Report. Cambridge University Press, IPCC, Geneva, Switzerland.
Joos, F., Gerber, S., Prentice, I.C., Otto-Bliesner, B.L., Valdes, P.J., 2004. Transient simulations of Holocene atmospheric carbon dioxide and terrestrial carbon since the last Glacial Maximum. Global Biogeochem. Cy. 18 (GB2002).
Kageyama, M., Braconnot, P., Bopp, L., Mariotti, V., Roy, T., Woillez, M.-N., Caubel, A., Foujols, M.-A., Guilyardi, E., Khodri, M., Lloyd, J., Lombard, F., Marti, O., 2013. Mid-Holocene and last Glacial Maximum climate simulations with the IPSL model. Part II: model-data comparisons. Clim. Dyn. 40, 2469–2495. https://doi.org/10.1007/s00382-012-1499-5.
Kleinen, T., Brovkin, V., Munhoven, G., 2016. Modelled interglacial carbon cycle dynamics during the Holocene, the Eemian and Marine Isotope Stage (MIS) 11. Clim. Past 12, 2145–2160.
Krinner, G., Viovy, N., de Noblet-Ducoudre, N., Ogee, J., Polcher, J., Friedlingstein, P., Ciais, P., Sitch, S., Prentice, I.C., 2005. A dynamic global vegetation model for studies of the coupled atmosphere-biosphere system. Global Biogeochem. Cy. 19 (GB1015).
Levavasseur, G., Vrac, M., Roche, D.M., Paillard, D., 2012. Statistical modelling of a new global potential vegetation distribution. Environ. Res. Lett. 7, 044019. https://doi.org/10.1088/1748- 9326/7/4/044019.
Levy, P.E., Friend, A.D., White, A., Cannell, M.G.R., 2004. The influence of land use change on global-scale fluxes of carbon from terrestrial ecosystems. Clim. Chang. 67, 185–209.
Liu, Y., Goodrick, S., Heilman, W., 2014. Wildland fire emissions, carbon, and climate: wildfire–climate interactions. Forest Ecol. Manag. 317, 80–96.
Long, S.P., 1991. Modification of the response of photosynthetic productivity to rising temperature by atmospheric CO_2 concentrations: has its importance been underestimated? Plant Cell Environ. 14 (8), 729–739.
Luo, Y., Su, B., Currie, W.S., Dukes, J.S., Finzi, A., Hertwig, U., Hungate, B., McMurtrie, R.E., Oren, R., Parton, W.J., Pataki, D.E., Shaw, M.R., Zak, D.R., Field, C.B., 2004. Progressive nitrogen limitation of ecosystem responses to rising atmospheric carbon dioxide. BioScience 54, 731–739.
Mayle, F.E., Langstroth, R.P., Fisher, R.A., Mair, P., 2007. Long term savannah dynamics in the Bolivian Amazon: implications for conservation. Philos. Trans. R. Soc. B 367, 291–307.
Medlyn, B.E., Barton, C.V.M., Broadmeadow, M.S.J., Ceulemans, R., De Angelis, P., Forstreuter, M., Freeman, M., Jackson, S.B., Kellomaki, S., Laitat, E., Rey, A., Roberntz, P., Sigurdsson, B.D., Strassemeyer, J., Wang, K., Curtis, P.S., Jarvis, P.G., 2001. Stomatal conductance of forest species after long-term exposure to elevated CO_2 concentration: a synthesis. New Phytol. 149 (2), 247–264.
Monserud, R.A., Leemans, R., 1992. Comparing global vegetation maps with the Kappa statistic. Ecol. Model. 62, 275–293.
New, M.G., Hulme, M., Jones, P.D., 2000. Representing twentieth century space-climate variability, Part II, Development of 1901–1996 monthly grids of terrestrial surface

climate. J. Clim. 13, 2217–2238.
Norby, R.J., DeLucia, E.H., Gielen, B., Calfapietra, C., Giardina, C.P., King, J.S., Ledford, J., McCarthy, H.R., Moore, D.J.P., Ceulemans, R., De Angelis, P., Finzi, A.C., Karnosky, D.F., Kubiske, M.E., Lukac, M., Pregitzer, K.S., Scarascia-Mugnozza, G.E., Schlesinger, W.H., Oren, R., 2005. Forest response to elevated CO_2 is conserved across a broad range of productivity. Proc. Natl. Acad. Sci. U. S. A. 102, 18052–18056.
Opsteegh, J.D., Haarsma, R.J., Selten, F.M., Kattenberg, A., 1998. ECBilt: a dynamic alternative to mixed boundary conditions in ocean models. Tellus A 50, 348–367.
Petoukhov, V., Ganopolski, A., Brovkin, V., Claussen, M., Eliseev, A., Kubatzki, C., Rahmstorf, S., 2000. CLIMBER-2: a climate system model of intermediate complexity, part I: Model description and performance for present climate. Clim. Dyn. 16, 1–17.
Pitman, A.J., 2003. The evolution of, and revolution in, land surface schemes designed for climate models. Int. J. Climatol. 23 (5), 479–510.
Pomeroy, J.W., Dion, K., 1996. Winter radiation extinction and reflection in a boreal pine canopy: Measurements and modelling. Hydrol. Process. 10, 1591–1608.
Prentice, I.C., Cramer, W., Harrison, S.P., Leemans, R., Monserud, R.A., Solomon, A.M., 1992. A global biome model based on plant physiology and dominance, soil properties and climate. J. Biogeogr. 19, 117–134.
Prentice, I.C., Harrison, S.P., 2009. Ecosystem effects of CO_2 concentration: evidence from past climates. Clim. Past 5, 297–307.
Prentice, I.C., Jolly, D., BIOME 6000 Participants, 2000. Mid-Holocene and glacial-maximum vegetation geography of the northern continents and Africa. J. Biogeogr. 27, 507–519.
Prentice, I.C., Bondeau, A., Cramer, W., Harrison, S.P., Hickler, T., Lucht, W., Sitch, S., Smith, B., Sykes, M.T., 2007. Chapter 15. In: Canadell, J., Pitelka, L., Pataki, D. (Eds.), Terrestrial Ecosystems in a Changing World. IGBP Book Seriespp. 175–192.
Prentice, I.C., Kelley, D.I., Foster, P.N., Friedlingstein, P., Harrison, S.P., Bartlein, P.J., 2011. Modeling fire and the terrestrial carbon balance. Global Biogeochem. Cy. 25, 1–13.
Quillet, A., Peng, C., Garneau, M., 2010. Toward dynamic global vegetation models for simulating vegetation-climate interactions and feedbacks: recent developments, limitations, and future challenges. Environ. Rev. 18, 333–353.
Raddatz, T.J., Reick, C.H., Knorr, W., Kattge, J., Roeckner, E., Schnur, R., Schnitzler, K.G., Wetzel, P., Jungclaus, J., 2007. Will the tropical land biosphere dominate the climate-carbon cycle feedback during the twenty-first century? Clim. Dyn. 29, 565–574.
Reick, C.H., Raddatz, T., Brovkin, V., Gayler, V., 2013. The representation of natural and anthropogenic landcover change in MPIESM. J. Adv. Model. Earth Syst. 5, 459–482.
Renssen, H., Brovkin, V., Fichefet, T., Goosse, H., 2006. Simulation of the Holocene climate evolution in Northern Africa: the termination of the African Humid Period. Quat. Int. 150, 95–102.
Roche, D.M., Dokken, T.M., Goosse, H., Renssen, H., Weber, S.L., 2007. Climate of the last Glacial Maximum: sensitivity studies and model-data comparison with the LOVECLIM coupled model. Clim. Past 3, 205–224.
Roche, D.M., Dumas, C., Bügelmayer, M., Charbit, S., Ritz, C., 2014. Adding a dynamical cryosphere to iLOVECLIM (version 1.0): coupling with the GRISLI ice-sheet model. Geosci. Model Dev. 7, 1377–1394.
Rossow, W.B., Walker, A.W., Beuschel, D.E., Roiter, M.D., 1996. International Satellite Cloud Climatology Project (ISCCP) Documentation of New Cloud Datasets, WMO/TD-No 737. World Meteorological Organisation.
Scheiter, S., Higgins, S.I., 2009. Impacts of climate change on the vegetationof Africa: an adaptive dynamic vegetation modelling approach. Glob. Chang. Biol. 15, 2224–2246.
Schurgers, G., Mikolajewicz, U., Groger, M., Maier-Reimer, E., Vizcaıno, M., Winguth, A., 2006. Dynamics of the terrestrial biosphere, climate and atmospheric CO_2 concentration during interglacials: a comparison between Eemian and Holocene. Clim. Past 2, 205–220. https://doi.org/10.5194/cp-2-205-2006.
Seddon, A.W.R., Macias-Fauria, M., Long, P.R., Benz, D., Willis, K.J., 2016. Sensitivity of global terrestrial ecosystems to climate variability. Nature 531, 229–232.
Silapaswan, C.S., Verbyla, D.L., McGuire, A.D., 2001. Land cover change on the Seward Peninsula: the use of remote sensing to evaluate the potential influences of climate warming on historical vegetation dynamics. Can. J. Remote. Sens. 27, 542–554.
Sitch, S., Smith, B., Prentice, I.C., Arneth, A., Bondeau, A., Cramer, W., Kaplan, J.O., Levis, S., Lucht, W., Sykes, M.T., Thonicke, K., Venevsky, S., 2003. Evaluation of ecosystem dynamics, plant geography and terrestrial carbon cycling in the LPJ dynamic global vegetation model. Glob. Chang. Biol. 9, 161–185.
Sitch, S., McGuire, A.D., Kimball, J., Gedney, N., Gamon, J., Engstrom, R., Wolf, A., Zhuang, Q., Clein, J., Mcdonald, K.C., 2007. Assessing the carbon balance of circumpolar Arctic tundra using remote sensing and process modelling. Ecol. Appl. 17, 213–234.
Sitch, S., Huntingford, C., Gedney, N., Levy, P.E., Lomas, M., Piao, S.L., Betts, R., Ciais, P., Cox, P., Friedingstein, P., Jones, C.D., Prentice, I.C., Woodwards, F.I., 2008. Evaluation of the terrestrial carbon cycle, future plant geography and climate-carbon cycle feedbacks using five Dynamic Global Vegetation Models (DGVMs). Glob. Chang. Biol. 14, 2015–2039.
Smith, B., Prentice, I.C., Sykes, M.T., 2001. Representation of vegetation dynamics in the modelling of terrestrial ecosystems: comparing two contrasting approaches within European climate space. Glob. Ecol. Biogeogr. 10, 621–637.
Smith, B., Wårlind, D., Arneth, A., Hickler, T., Leadley, P., Siltberg, J., Zaehle, S., 2014. Implications of incorporating N cycling and N limitations on primary production in an individual-based dynamic vegetation model. Biogeosciences 11, 2027–2054.
Stow, D.A., Hope, A., McGuire, A.D., Verbyla, D., Gamon, J., Huemmrich, F., Houston, S., Racine, C., Sturm, M., Tape, K., Hinzman, L., Yoshikawa, K., Tweedie, C., Noyle, B., Silapaswan, C., Douglas, D., Griffith, B., Jia, G.S., Epstein, H., Walker, D., Daeschner, S., Petersen, A., Zhou, L.M., Myneni, R., 2004. Remote sensing of vegetation and land- cover change in Arctic tundra ecosystems. Remote Sens. Environ. 89, 281–308.
Sturm, M., Racine, C., Tape, K., 2001. Increasing shrub abundance in the Arctic. Nature 411, 546–547.
Warnant, P., Francois, L., Strivay, D., Gérard, J.C., 1994. CARAIB: a global model of terrestrial biological productivity. Global Biogeochem. Cy. 9, 255–270.
Wenzel, S., Cox, P.M., Eyring, V., Friedlingstein, P., 2014. Emergent constraints on climate–carbon cycle feedbacks in the CMIP5 Earth system models. J. Geophys. Res. Biogeosci. 119, 794–807.
Woillez, M.N., Kageyama, M., Krinner, G., de Noblet-Ducoudré, N., Viovy, N., Mancip, M., 2011. Impact of CO_2 and climate on the last Glacial Maximum vegetation: results from the ORCHIDEE/IPSL models. Clim. Past 7, 557–577.
Woodward, F.I., Cramer, W., 1996. Plant functional types and climatic changes: Introduction. J. Veg. Sci. 7 (3), 306–308.
Woodward, F.I., Kelly, C.K., 1995. The influence of CO_2 concentration on stomatal density. New Phytol. 131, 311–327.
Woodward, F.I., Lomas, M.R., 2004. Vegetation-dynamics – simulating responses to climate change. Biol. Rev. 79, 643–670.
Zaehle, S., Dalmonech, D., 2011. Carbon-nitrogen interactions on land at global scales: current understanding in modelling climate biosphere feedbacks. Curr. Opin. Environ. Sustain. 3, 311–320.
Zhu, Z., Piao, S., Myneni, R.B., Huang, M., Zeng, Z., Canadell, J.G., Ciais, P., Sitch, S., Friedlingstein, P., Arneth, A., Cao, C., Cheng, L., Kato, E., Koven, C., Li, Y., Lian, X., Liu, Y., Liu, R., Mao, J., Pan, Y., Peng, S., Peñuelas, J., Poulter, B., Pugh, T.A.M., Stocker, B.D., Viovy, N., Wang, X., Wang, Y., Xiao, Z., Yang, H., Zaehle, S., Zeng, N., 2016. Greening of the Earth and its drivers. Nat. Clim. Chang. 1–6.